

2010

# Performance of a pilot scale biomass gasification and producer gas combustion system using feedstock with controlled nitrogen content

Sharan Sethuraman  
*Iowa State University*

Follow this and additional works at: <https://lib.dr.iastate.edu/etd>



Part of the [Mechanical Engineering Commons](#)

## Recommended Citation

Sethuraman, Sharan, "Performance of a pilot scale biomass gasification and producer gas combustion system using feedstock with controlled nitrogen content" (2010). *Graduate Theses and Dissertations*. 11725.  
<https://lib.dr.iastate.edu/etd/11725>

This Thesis is brought to you for free and open access by the Iowa State University Capstones, Theses and Dissertations at Iowa State University Digital Repository. It has been accepted for inclusion in Graduate Theses and Dissertations by an authorized administrator of Iowa State University Digital Repository. For more information, please contact [digirep@iastate.edu](mailto:digirep@iastate.edu).

**Performance of a pilot scale biomass gasification and producer gas  
combustion system using feedstock with controlled nitrogen content**

by

**Sharan Sethuraman**

A thesis submitted to the graduate faculty in partial fulfillment of the

requirements for the degree of

MASTER OF SCIENCE

Major: Mechanical Engineering

Program of Study Committee:

Song-Charng Kong, Major Professor

Terrence Meyer

Gap Yong Kim

Iowa State University

Ames, Iowa

2010

## TABLE OF CONTENTS

LIST OF FIGURES.....	iv
LIST OF TABLES.....	vi
ACKNOWLEDGEMENT.....	vii
ABSTRACT.....	viii
CHAPTER 1. INTRODUCTION.....	1
1.1 Motivation.....	1
1.2 Objective.....	3
CHAPTER 2. LITERATURE REVIEW.....	4
2.1 Introduction.....	4
2.2 Gasification process.....	5
2.3 Coal gasification.....	6
2.3.1 Introduction.....	6
2.3.2 Process.....	6
2.3.3 Lurgi slagging gasifier.....	8
2.4 Biomass Gasification.....	9
2.4.1 Introduction.....	9
2.4.2 Types of biomass gasifiers.....	11
2.5 Effect of biomass feedstock on the gas composition.....	13
2.6 Gas clean-up technologies.....	19
2.7 Fate of nitrogen in biomass feedstock.....	22
2.7.1 Introduction.....	22
2.7.2 Fuel NO <sub>x</sub> chemistry.....	24
2.7.3 Comparison of thermal NO <sub>x</sub> and fuel NO <sub>x</sub> .....	26
2.8 Producer gas combustion.....	29
2.8.1 Differences between syngas and producer gas.....	29
2.8.2 Status of producer gas combustion research.....	30
2.8.3 Low BTU Burner.....	33
CHAPTER 3: METHODS AND PROCEDURES.....	36
3.1 Introduction.....	36
3.2 BECON gasification system.....	36

3.3 COMBUSTION SYSTEM .....	40
3.4 Producer gas analysis .....	43
3.4.1 Micro gas chromatograph (GC) .....	43
3.4.2 International Energy Agency (IEA) tar protocol .....	44
3.4.3 Moisture analysis .....	50
3.4.4 Tar and ammonia separation .....	50
3.4.5 Ammonia analysis .....	53
CHAPTER 4: RESULTS AND DISCUSSIONS .....	56
4.1 Test matrix .....	56
4.2 Producer gas compositions .....	58
4.3 Emissions using natural gas .....	59
4.4 Emissions using wood .....	63
4.5 Emissions using wood with 7% DDGS .....	65
4.6 Emissions using wood with 13% DDGS .....	67
4.7 Emissions using wood with 20% DDGS .....	69
4.8 Emissions using wood with 40% DDGS .....	71
4.9 Emissions using wood with 70% DDGS .....	73
4.9 Emissions using yellow corn .....	75
4.11 Discussions .....	77
CHAPTER 5: CONCLUSIONS AND RECOMMENDATIONS .....	86
5.1 Conclusions .....	86
5.2 Future recommendations .....	87
APPENDIX A1. ENGINEERING EQUATION SOLVER (EES) CODE .....	89
BIBLIOGRAPHY .....	91

## LIST OF FIGURES

Fig 2.1 - Schematic of coal gasification process .....	8
Fig 2.2 - Schematic of OLGA technique .....	20
Fig 2.3 - Conversion of fuel bound nitrogen in biomass .....	24
Fig 2.4 - Ammonia formation at different gasification temperatures for cane trash .....	27
Fig 2.5 - Laminar flame speed for CO/H <sub>2</sub> mixtures at different pressures.....	30
Fig 2.6 - Effect of adiabatic flame temperature on CO and NO <sub>x</sub> emissions.....	32
Fig 2.7 - NO <sub>x</sub> emissions for different flames with and without EGR.....	33
Fig 2.8 - Schematic representation of low NO <sub>x</sub> burner process .....	35
Fig 3.1 - Bubbling fluidized bed gasifier at Becon .....	36
Fig 3.2 - Feed auger with screw operated mechanism .....	37
Fig 3.3 - Char collected at the bottom of the baghouse .....	38
Fig 3.4 - Schematic representation of the gasification and the combustion system.....	39
Fig 3.5 - Combustion chamber surrounding the burner .....	41
Fig 3.6 - Point of entry for fuel and air .....	42
Fig 3.7 - Scheme of the sampling line for the IEA tar protocol .....	44
Fig 3.8 - IEA setup with the three impingers downstream .....	46
Fig 3.9 - IEA sampling method.....	47
Fig 3.10 - Sampling and analysis procedure .....	48
Fig 3.11 - Roto-evap system with a chiller (left) and the samples equally distributed in six flasks (right) .....	51
Fig 3.12 - Tars after the distillation process .....	51
Fig 3.13 - Calibration curve on the UV-Vis spectrophotometer.....	53
Fig 3.14 - Thermo scientific NO <sub>x</sub> analyzer.....	54
Fig 4.1 - NO <sub>x</sub> variation with equivalence ratio for different heat rates using natural gas.....	62
Fig 4.2 - NO <sub>x</sub> emissions using producer gas resulting from gasifying wood .....	64
Fig 4.3 - NO <sub>x</sub> emissions using producer gas resulting from gasifying wood with 7% DDGS.....	66
Fig 4.4 - NO <sub>x</sub> emissions using producer gas resulting from gasifying wood with 13% DDGS.....	68
Fig 4.5 - NO <sub>x</sub> emissions using producer gas resulting from gasifying wood with 20% DDGS.....	70
Fig 4.6 - NO <sub>x</sub> emissions using producer gas resulting from gasifying wood with 40% DDGS.....	72

Fig 4.7 - NO <sub>x</sub> emissions using producer gas resulting from gasifying wood with 70% DDGS.....	74
Fig 4.8 - NO <sub>x</sub> emissions using producer gas resulting from gasifying yellow corn .....	76
Fig 4.9 - Effect of fuel nitrogen on NO <sub>x</sub> emissions for producer gas flow rate of 150 pph .....	78
Fig 4.10 - Change in NO <sub>x</sub> for different nitrogen contents in the biomass feedstock.....	82
Fig 4.11 - Relation of nitrogen content, ammonia and NO <sub>x</sub> emissions for producer gas flow rate of 150 pph and equivalence ratio of 1.65 .....	84
Fig 4.12 – NO <sub>x</sub> vs NH <sub>3</sub> .....	85

**LIST OF TABLES**

Table 2.1 - Syngas from coal gasification process.....	9
Table 2.2 - Proximate and ultimate analysis for seed corn.....	14
Table 2.3 - Producer gas composition for seed corn.....	15
Table 2.4 - Producer gas for olive oil waste.....	16
Table 2.5 - Producer gas composition for wood.....	17
Table 2.6 - Ultimate and proximate analysis of miscanthus pellets.....	18
Table 2.7 - Raw producer gas composition for miscanthus pellets.....	19
Table 2.8 - Fuel nitrogen distribution in the resultant producer gas.....	23
Table 4.1 - Test Conditions.....	57
Table 4.2 - Proximate and ultimate analysis of different biomass feedstock.....	57
Table 4.3 - Producer gas composition using different biomass feedstock.....	59

## ACKNOWLEDGEMENT

I would like to first thank my major professor Dr. Song-Charng Kong for this unique opportunity to work in such a novel project. He has guided me throughout my Master's program at Iowa State University and has been a source of inspiration. I would extend my sincere gratitude towards Dr. Terrence Meyer, who along with Dr. Song-Charng Kong has provided exceptional support during my program. I would also like to thank Dr. Gap-Yong Kim for serving as my committee member.

I would like to acknowledge Iowa Office of Energy Independence for their financial support. I would also like to thank Patrick Johnston, Dr. Robert Brown, John Reardon, Jerod Smeenk, and Adam Kufner for their engineering support and sharing their wealth of experience and knowledge.

I would like to thank all the graduate students in Dr. Kong's group, whose help made my journey towards my Master's degree a smooth ride. In particular, I would like to show my appreciation to Coung Van Huynh, Johannes Ruf, Matthias Veltman, Sujith Sukumaran, and Jordan Tiarks. I would also like to thank the undergraduate research assistant Nicholas Poduska. Their help and support has made my experience at Iowa State University a truly memorable one.

Finally, I would like to thank my family back in India and my friends. They have always been with me through my thick and thin, and I would dedicate my thesis work to them.

## ABSTRACT

This study is focused on the effects of nitrogen content in biomass feedstock on the producer gas composition and the flue gas NO<sub>x</sub> emissions from a pilot-scale gasification and combustion system. Biomass gasification has the potential to produce carbon negative energy by using renewable resources. The greenhouse gases emitted by burning fossil fuels have to be reduced, and biomass gasification is one of the means to achieving this. When the biomass-derived gas is burned, NO<sub>x</sub> emissions are a critical factor that can limit the use of the system. The government regulations limit the amount of NO<sub>x</sub> that can be emitted into the atmosphere. These emission regulations are becoming more stringent every year. Hence it is imperative to design combustion systems that can produce low NO<sub>x</sub> emissions without compromising the intended purpose for heat and power generation. This work is aimed at helping with the design of a low NO<sub>x</sub> burner by conducting experimental investigations on an existing burner.

In this study, tests were conducted in a pilot-scale fluidized bed gasifier using biomass feedstock with different nitrogen contents. The producer gas from the gasifier undergoes a gas cleaning phase before its combustion in a burner. Fuel NO<sub>x</sub> and thermal NO<sub>x</sub> contributed to the total NO<sub>x</sub> formation in the burner. The main precursor to fuel NO<sub>x</sub> is ammonia in the producer gas. Ammonia and tars were collected from the producer gas using IEA (International Energy Agency) tar protocol and analyzed using spectrophotometer and GC-FID (Gas chromatograph-flame ionization detector), respectively. The producer gas and the exhaust flue gas were analyzed using a micro gas chromatograph (Micro-GC). The

NO<sub>x</sub> variation was investigated for different equivalence ratios and different flow rates of the producer gas.

Results show that there is a direct and proportional relationship between nitrogen in biomass, ammonia in producer gas, and NO<sub>x</sub> in the flue gas. Additionally, NO<sub>x</sub> emissions do not vary noticeably with the overall equivalence ratio in the present burner but vary significantly with increased heat rate. It was also found that thermal NO<sub>x</sub> is less significant than fuel NO<sub>x</sub>, which constitutes a majority of the total NO<sub>x</sub> emissions when biomass-derived producer gas is used. The flame length in a diffusion flame along with the residence time seems to have a major influence on the NO<sub>x</sub> emissions from the burner.

These results form an essential part in understanding the fuel NO<sub>x</sub> behavior and functions as an important tool in the development of a low NO<sub>x</sub> burner, which was the overall objective of this project. This thesis work is mainly focused on the experimental investigation of the fuel NO<sub>x</sub> behavior and the effect of fuel nitrogen on the NO<sub>x</sub> formation in the burner. These experimental results along with detailed chemical analysis of ammonia oxidation mechanisms under different conditions will give a better understanding of the fuel NO<sub>x</sub> formation and will aid in the design of low NO<sub>x</sub> burners.

## CHAPTER 1. INTRODUCTION

### 1.1 Motivation

The use of renewable energy is essential to alleviate global warming (McKendry 2002). Renewable energy can play a major role in reducing greenhouse gas emissions resulting from burning fossil fuels (Babu 2006). Unlike fossil fuel, biomass is a renewable energy resource that can potentially produce zero net carbon dioxide emissions (Tijmensen, Faaij et al. 2002). Biomass energy or bio-energy is the energy derived from plants or plant-derived materials. Biomass is one of the renewable energy sources with a great potential to produce energy carriers such as transportation fuels and electricity, in addition to being carbon neutral (Ptasinski, Prins et al. 2007). The technological advancements have led to increased applications of biomass at comparatively lower costs and higher conversion efficiencies than previously possible. Biomass can be converted to gaseous or liquid fuels by thermo-chemical or bio-chemical processes (Darvell 2006). While the thermo-chemical conversion takes place at elevated temperature and pressure conditions, the bio-chemical conversion uses sophisticated fermentation processes to produce valuable liquid fuels. Biomass gasification is one of the few technologies that can potentially generate carbon negative energy with pollution-free power and also turn agricultural waste into energy. Biomass gasification is a thermo-chemical process that generates producer gas or synthesis gas by the partial oxidation of the biomass feedstock in fuel-rich conditions in the presence of air, steam, or oxygen (Li, Grace et al. 2004). Notice that “producer gas,” rather than “synthesis gas,” is the biomass derived gas used in this research. The gasification

technology has received attention due to the following advantages. First, the introduction of a new biomass feedstock requires little or no change to the system. Additionally, the resulting gases can be used in various applications such as heat and power generation or synthesis to produce liquid fuels (Chen et al. 2007). Another advantage is that the electricity production via biomass gasification can produce less exhaust emissions, as compared to coal. Thermo-chemical gasification can be classified on the basis of the gasifying agent, which could be air, steam, or oxygen (Lv, Xiong et al. 2004). Air blown gasification processes usually yield a low calorific value gas with a higher heating value (HHV) of 4 – 7 MJ/Nm<sup>3</sup>. Oxygen and steam blown gasification usually yield gases with a HHV of 10 – 18 MJ/Nm<sup>3</sup>. The disadvantage with the oxygen blown system is the high cost for the oxygen production equipment. The four popular gasifiers are downdraft, updraft, fluidized bed, and entrained flow. For large-scale applications, the most preferred and reliable system is the circulating fluidized bed, while for small scale systems, downdraft systems are more appropriate (Maniatis 2001).

Nitrogen in biomass feedstock is converted to nitrogen-containing compounds such as ammonia (NH<sub>3</sub>) and hydrogen cyanide (HCN) during the gasification process. It has been shown that ammonia is the dominant nitrogen-containing compound in producer gas during the gasification of biomass (Tian, Yu et al. 2007). Ammonia is an important concern as it is the precursor to NO<sub>x</sub> emissions when producer gas is combusted in a burner or an internal combustion engine. Hence an accurate assessment of the quantity of ammonia is a key to controlling NO<sub>x</sub> emissions. As the emissions regulation becomes stringent, it is essential to reduce NO<sub>x</sub> emissions in order for biomass gasification to be viable. In theory,

NO<sub>x</sub> emissions include thermal NO<sub>x</sub> (due to high temperature), fuel NO<sub>x</sub> (due to fuel-bound nitrogen), and prompt NO<sub>x</sub> (due to fuel rich conditions) (Turns, 2000). During biomass gasification, nitrogen in biomass is released as ammonia, whose combustion will lead to significant NO<sub>x</sub> emissions, especially fuel NO<sub>x</sub> (Waibel 1993). Therefore, the relationship between nitrogen content in biomass feedstock and NO<sub>x</sub> emissions from producer gas combustion needs to be investigated.

## 1.2 Objective

The purpose of this work is to investigate the effects of biomass feedstock on producer gas composition and exhaust NO<sub>x</sub> emissions in a pilot-scale biomass gasifier integrated with an industrial burner. Different biomass feedstocks with varying nitrogen contents were tested. It is believed that biomass with higher nitrogen content will result in more ammonia in the producer gas which, in turn, will produce higher NO<sub>x</sub> emissions in the flue gas (Li and Tan 2000). The goal of this work is to help understand the relationship between the fuel-bound nitrogen in the feedstock to ammonia formation in the producer gas and hence the NO<sub>x</sub> emissions from the burner.

## CHAPTER 2. LITERATURE REVIEW

### 2.1 Introduction

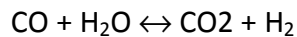
Gasification is a process that converts carbonaceous materials such as coal, petroleum, bio-fuel or biomass into carbon monoxide, hydrogen and other hydrocarbons by subjecting the raw material to a high temperature, with controlled amount of oxygen or steam. The amount of oxygen is less than that required for complete combustion, and the addition of steam is to increase hydrogen production in the resulting gas product. The resulting gas mixture is called synthesis gas or syngas and is itself a fuel. Gasification is a method for extracting energy from many different types of organic materials whose direct combustion is not favorable. The advantage of gasification is that using the syngas is potentially more efficient than direct combustion of the original fuel because it can be combusted at higher temperatures or even in fuel cells, so that the thermodynamic upper limit to the efficiency defined by Carnot's rule is higher or not applicable. Syngas may be burned directly in internal combustion engines, used to produce methanol and hydrogen, or converted via the Fischer-Tropsch process into synthetic fuel. Gasification can also begin with materials that are not otherwise useful fuels, such as biomass or organic waste. In addition, the high-temperature combustion refines out corrosive ash elements such as chloride and potassium, allowing clean gas production from otherwise problematic fuels. Gasification relies on chemical processes at elevated temperatures ( $>700^{\circ}\text{C}$ ), which distinguishes it from biological processes such as anaerobic digestion that produce biogas (Chen, 2007).

## 2.2 Gasification process

In a gasifier, the carbonaceous material undergoes several different processes:

- **Pyrolysis** : In this process the carbonaceous material heats up. Volatiles are released and char is produced, resulting in up to 70% weight loss for coal. The process is dependent on the properties of the carbonaceous material and determines the structure and composition of the char, which will then undergo gasification reactions.
- **Combustion**: In this process the volatile products and some of the char reacts with oxygen to form carbon dioxide and carbon monoxide, which provides subsequent heat for the gasification reaction.
- **Gasification**: The char reacts with the carbon dioxide and steam to form carbon monoxide and hydrogen.

Also the reversible gas phase water gas shift reaction reaches equilibrium very fast at the temperatures in a gasifier. This balances the concentrations of carbon monoxide, steam, carbon dioxide and hydrogen. The water gas shift reaction is as follows.



## 2.3 Coal gasification

### 2.3.1 Introduction

Coal gasification was first developed in about 1780 and was widely commercialized by the early 1900s. Before natural gas became widely available in the 1940s, many European and North American nations used town gas or producer gas derived from coal as a heating and lighting fuel. Later natural gas replaced producer gas because of its high heating value. The oil crisis of 1970s triggered a renewed interest in various coal utilization technologies like the coal gasification, in order to replace or compete with the petroleum resources such as oil or natural gas.

### 2.3.2 Process

The coal gasification process involves several stages before the actual gasification process can take place. The raw coal after preparation is introduced by a feeding system into the gasification reactor. The coal minerals, which remain as ash or slag, after the gasification process, are discharged and used for purposes such as the construction of buildings or roads, or disposed. The solids in the raw gas are either treated like the ash or if they contain considerable amounts of un-gasified carbon, they are recycled into the gasifier. There are different possibilities of heat being transferred to the gasifier. One is auto thermal coal gasification process in which the reaction heat is generated in the gasifier itself by using as a gasifying agent a mixture of oxygen and steam, whereby a certain amount of coal is burnt and the remainder reacts with steam. Second is the allo-thermal

coal gasification in which the heat is generated outside the gasifier by burning either coal or its products in a separate combustion chamber with air. The heat can be transferred to the gasifier either by superheated steam, steam/gas mixtures or by solid heat carriers.

In the case of an autothermic process, gasification is performed with steam and oxygen, the latter being produced by a cryogenic air separation process. A schematic diagram of the coal gasification process is shown in Fig 2.1 (Nowacki, 1981).

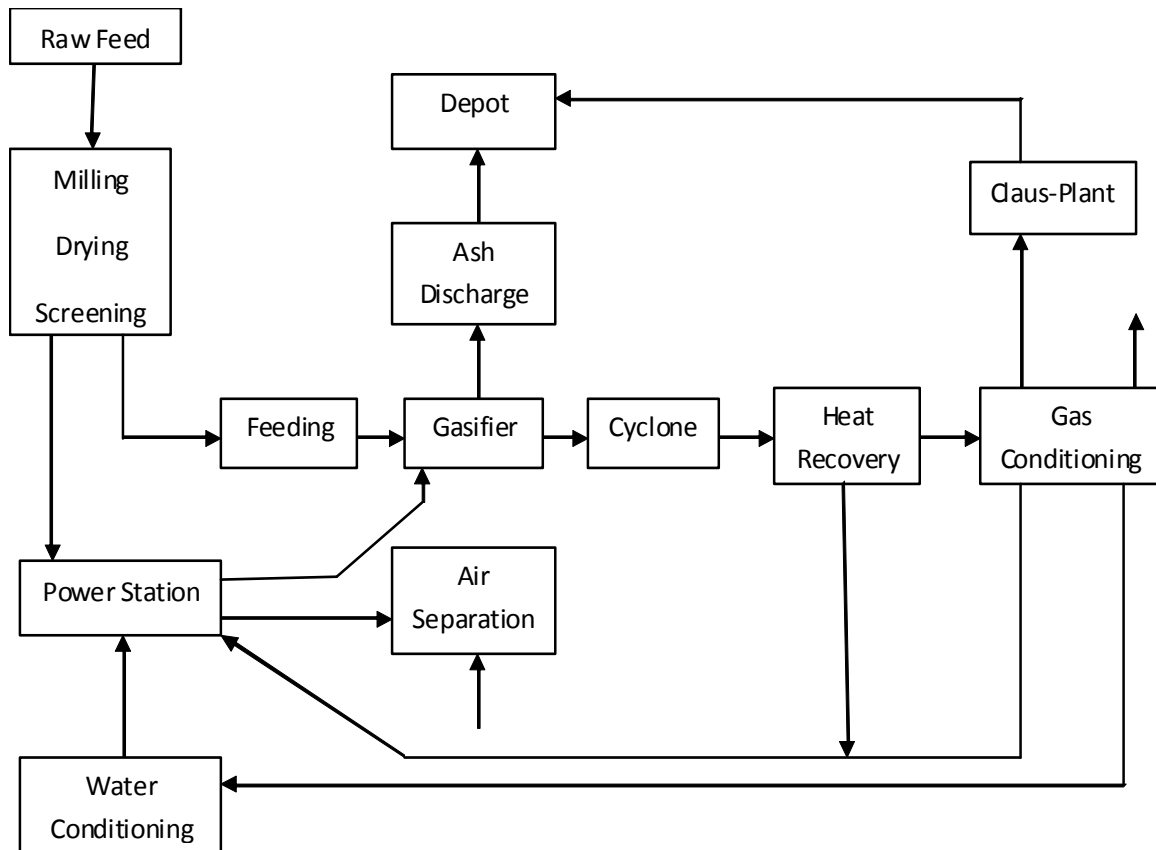


Fig 2.1 Schematic diagram of a coal gasification process

In a fixed or moving bed gasifier a bed of coal particles is moving downwards in a countercurrent flow of oxygen and steam. In order to attain reasonable gasification rates the gas velocity must be high and the pressure drop low. The product gas leaving the gas generator at the top contains pyrolysis products which are formed in the upper layer of the fixed bed. Most processes use a dry ash removal, thus the reaction temperatures must be below the fusion point of the ash. The raw gas is de-dusted, cooled down and finally purified and thus converted into a feedstock for following synthesis or other utilization. Gas purification and processing consists of a high number of washers and other chemical apparatus. The gas purification and processing account for about 60% of investment cost and hence is of high significance.

The typical gas compositions from the coal gasification depends on the kind of gasifier, the operating conditions like temperature, pressure, residence time and the gas velocity. The following mentions the producer gas composition in a Lurgi slagging gasifier under a given operating condition (Nowacki, 1981).

### **2.3.3 Lurgi slagging gasifier**

**Type of gasifier:** Fixed bed gasifier

**Temperature:** Combustion zone temperatures are around 2300 – 2500<sup>0</sup> F

**Pressure:** 5 – 26 atm

**Gas velocity/Residence time:** Gas velocity is approximately 2.5 fps above the slag bath. The coal residence time is about 10 to 15 min.

The syngas composition resulting from the coal gasification process is shown in Table 2.1

**Table 2.1 - Syngas from coal gasification process**

Composition	Vol %
H <sub>2</sub>	28.05
CO	61.20
CO <sub>2</sub>	2.55
CH <sub>4</sub>	7.65
C <sub>n</sub> H <sub>m</sub>	0.45
O <sub>2</sub>	0.10
Heating value (HHV), Btu/scf	381

## 2.4 Biomass Gasification

### 2.4.1 Introduction

Biomass gasification is the conversion of solid biomass into a combustible gas mixture usually of low heating value, by the partial oxidation of biomass at high temperatures, at atmospheric or elevated pressures. The gasification of biomass is carried out mainly via partial oxidation processes and steam reforming. Partial oxidation processes are those that utilize less than the stoichiometric amount of oxygen needed for complete oxidation, so partially oxidized products like carbon monoxide (CO) and higher hydrocarbons are formed. This gas mixture is called the producer gas or synthesis gas depending on the conditions run at the gasifier side. The producer gas or synthesis gas can be used in different

applications such as burning it to produce heat or it can be used to produce electricity, if used as a fuel for gas engines and gas turbines. It has been estimated that the overall efficiency of conversion of biomass to energy using gasification and pyrolysis is 70-75% (Ptasinski, 2008).

Biomass gasification is one of the few technologies that can potentially generate carbon negative energy with pollution-free power and also turn agricultural waste into energy. Biomass gasification is a thermochemical process that generates producer gas or synthesis gas by the partial oxidation of the biomass feedstock in fuel-rich conditions in the presence of air, steam, or oxygen (Li et al. 2004). Notice that “producer gas,” rather than “synthesis gas,” will be used in this article to describe the biomass-derived gas. The gasification technology has received attention due to the following advantages. First, the introduction of a new biomass feedstock requires little or no change to the system. Additionally, the resulting gases can be used in various applications such as heat and power generation or synthesis to produce liquid fuels (Chen et al. 2007). Another advantage is that the electricity production via biomass gasification can produce less exhaust emissions, as compared to coal. Thermo-chemical gasification can be classified on the basis of the gasifying agent, which could be air, steam, or oxygen (Lv, Xiong et al. 2004). Air blown gasification processes usually yield a low calorific value gas with a higher heating value (HHV) of 4 – 7 MJ/Nm<sup>3</sup>. Oxygen and steam blown gasification usually yield gases with a HHV of 10 – 18 MJ/Nm<sup>3</sup>. The disadvantage with the oxygen blown system is the high cost for the oxygen production equipment. The four popular gasifiers are downdraft, updraft,

fluidized bed, and entrained flow. For large-scale applications, the most preferred and reliable system is the circulating fluidized bed, while for small scale systems, downdraft systems are more appropriate (Maniatis, 2001).

#### **2.4.2 Types of biomass gasifiers**

Mainly there are two types of gasifiers that are used. They are fixed bed gasifiers and fluidized bed gasifiers. The fixed beds suffer localized hot spots and thus have a wide temperature distribution. This includes possibilities for hot spots with ash fusion, low specific capacity, long periods for heat-up and a limited scale-up potential. Scaling up of a fixed bed gasification plant is unfeasible as it includes higher investment costs for a cascade of single fixed beds. The main advantages are the high carbon efficiency, the wide range of ash content in the feedstock and the possibility to melt ash. Furthermore, concurrent fixed beds produce a clean gas with very low tar content. Fluidized beds have good heat and material transfer between the gas and solid phases with uniform temperature distribution, high specific capacity and fast heat-up. They tolerate wide variations in fuel quality and a broad particle-size distribution. Disadvantages of fluidized beds are high dust content in the gas phase and the conflict between high reaction temperatures with good conversion efficiency and low melting points of ash components.

There are mainly three types of fixed bed gasifiers.

**Updraft gasifiers:** In this system the oxidant is introduced at the bottom of the reactor and the fuel gas produced moves up through a bed of solid feedstock, which gradually moves down as the feed at the bottom is consumed. The gas tends to leave the gasifier at low temperature, because it has percolated through the bed, and therefore contains a fair fraction of lower molecular weight hydrocarbons and tar.

**Downdraft gasifiers:** In this system, the oxidant is introduced into a downward flowing packed bed of solid biomass and the product gas is drawn off at the bottom. Unlike the updraft gasifier, the product gas leaves the gasifier at high temperature, since it exits the reactor at the combustion zone, and hence resulting in an increased concentration of hydrogen and light hydrocarbons and less tar. This gasifier is preferred to updraft for internal combustion engines (Ragnar, 2000).

**Cross-flow gasifiers:** In this system, the biomass moves downwards while the air is introduced from the side, and the gases exit the gasifier on the opposite side, at the same level. Because a combustion zone forms around the entrance of air, this results in gases leaving the vessel at a relatively high temperature, hence lowering the overall energy efficiency.

There are mainly two kinds of fluidized bed gasifiers commercially used.

**Circulating fluidized bed:** In this system, the bed material is circulated between the unit and a cyclone separator, which removes the ash, and returns the bed material and char to

the gasifier. These gasifiers can be operated at higher pressures; hence it can be used in gas turbine applications.

**Bubbling bed gasifier:** In this gasifier, the air is introduced through a grate at the bottom, and the feed is introduced above the grate into the moving bed of fine-grained material, where it is pyrolysed forming a char with gaseous compounds. This results in a gas with low tar content, since the high molecular weight compounds are cracked by the hot bed material (Ragnar, 2000).

## 2.5 Effect of biomass feedstock on the gas composition

Typical producer gas compositions obtained from the biomass gasification process are outlined below. These compositions are analyzed just before the purification process. The conditions under which the producer gas is produced are also described below.

1. Tests were conducted at the Biomass Energy conversion facility (BECON) in Nevada, IA by the Iowa Energy Center. A pilot scale circulating fluidized bed reactor was used to conduct the experiments. The system is rated at 800kW thermal input, which corresponds to 180 kg/hr of solid biomass fuel with a heating value of 16000 kJ/kg. The gasifier was operated at an equivalence ratio between 0.25 and 0.35, which maintained the reactor in the range of 700 -760<sup>0</sup> C. The experiments employed discard seed corn as a fuel. The chemical composition of the fuel is as shown in Table 2.2 (Nowacki, 1981).

**Table 2.2 - Proximate and ultimate analysis for seed corn**

Items	Seed Corn
<b>Proximate analysis (wt %)</b>	
Fixed Carbon	11.7
Volatile	77.90
Moisture	9.00
Ash	1.40
<b>Ultimate Analysis (wt %)</b>	
C	41.7
O	49.24
H	6.43
N	1.1
S	0.13
Cl	0.17 ± 0.043
Ash	2.5 ± 0.44
<b>High Heating value (MJ/kg)</b>	17.6

Reference: Riquin Zhang, Robert.C. Brown, Andrew Suby, Keith Cumber. Catalytic destruction of tar in biomass derived producer gas – Energy Conversion and Management 45 (2004) 995–1014.

The average raw producer gas composition on dry volumetric basis is shown in Table 2.3.

Since the oxidizing agent is air, the heating value of the producer gas obtained is low, as indicated by the high nitrogen content.

**Table 2.3 - Producer gas composition for seed corn**

Constituent of producer gas	% Dry Volumetric basis
Nitrogen (N <sub>2</sub> )	51.2
Carbon Monoxide (CO)	15.7
Hydrogen (H <sub>2</sub> )	6.5
Carbon dioxide (CO <sub>2</sub> )	14.2
Methane (CH <sub>4</sub> )	4.8
Higher Hydrocarbons	4.0

Reference: Riquin Zhang, Robert.C. Brown, Andrew Suby, Keith Cummer. Catalytic destruction of tar in biomass derived producer gas – Energy Conversion and Management 45 (2004) 995–1014.

2. Tests were conducted on leached orujillo (olive oil waste) in a pilot plant circulating fluidized bed reactor. The experiments were conducted for different equivalence ratios at a temperature of about 800<sup>0</sup> C. It is seen that as the equivalence ratio is increased, the lower heating value of producer gas decreases, as there is more air utilized in the gasification process and hence higher nitrogen content in the resulting producer gas composition (Bridgwater, 2006). The dry producer gas composition by percentage volume for various equivalence ratios are as shown in the Table 2.4. It has to be noted that the nitrogen percentages increase with increasing equivalence ratio.

**Table 2.4 - Producer gas for olive oil waste**

<b>Constituent of producer gas</b>	<b>Test 1</b>	<b>Test 2</b>	<b>Test 3</b>	<b>Test 4</b>
Equivalence ratio	0.41	0.73	0.59	0.67
Nitrogen (N <sub>2</sub> ) (%)	59.46	63.16	60.55	62.46
Carbon Monoxide (CO)	8.6	6.9	8.4	7.5
Hydrogen (H <sub>2</sub> ) (%)	5.4	7.3	9.3	7.6
Carbon dioxide (CO <sub>2</sub> ) (%)	21.7	19.9	19.0	19.7
Methane (CH <sub>4</sub> ) (%)	3.0	1.8	1.9	1.8
Higher Hydrocarbons (%)	1.9	0.9	1.0	1.1

3. The following is a research conducted to clean the producer gas for I.C engine applications. This composition of producer gas is obtained from atmospheric air blown gasifiers. Tests were conducted with wood chips as the biomass feedstock. Three different types of gasifiers were tested for their producer gas compositions. One is the fixed bed concurrent gasifier, second being fixed bed counter-current gasifier and the third one is the circulating fluidized bed gasifier. The dry producer gas compositions are shown in Table 2.5 (Hasler, 1999).

**Table 2.5 - Producer gas composition for wood**

<b>Constituent of Producer gas</b>	<b>Fixed bed concurrent</b>	<b>Fixed bed Countercurrent gasifier</b>	<b>CFB gasifier</b>
Nitrogen (N <sub>2</sub> )	35 – 60	53 – 65	45 - 56
Carbon Monoxide	10 – 22	15 – 20	13 - 15
Hydrogen (H <sub>2</sub> )	15 – 21	10 – 14	15 - 22
Carbon dioxide	11 – 13	8 – 10	13 - 15
Methane (CH <sub>4</sub> )	1 – 5	2 – 3	3 - 4
Higher hydrocarbons	0.5 - 2	-	0.1 – 1.2

Reference : P. Hasler, Th. Nussbaumer. Gas cleaning for IC engine applications from fixed bed biomass gasification – Biomass and Bioenergy 16 (1999) 385 – 395.

4. This research involved combining the fast pyrolysis process and the gasification process to produce high quality producer gas. The producer gas is formed in a circulating fluidized bed reactor, which consists of a cyclone, riser, fuel feeder and a pre-heater. The raw fuel used is miscanthus pellet, the properties of which are shown in Table 2.6 (Chen, 2004).

**Table 2.6 - Ultimate and proximate analysis of miscanthus pellets**

<b>Items</b>	<b>Miscanthus pellet</b>
<b>Proximate analysis (wt %)</b>	
Fixed Carbon	15.0 ± 3.50
Volatile	73.8 ± 3.50
Moisture	8.70 ± 1.47
Ash	2.5 ± 0.44
<b>Ultimate Analysis (wt %)</b>	
C	43.9 ± 0.95
O	46.8 ± 0.81
H	5.90 ± 0.40
N	0.57 ± 0.12
S	0.14 ± 0.049
Cl	0.17 ± 0.043
Ash	2.5 ± 0.44
<b>High Heating value (MJ/kg)</b>	17.6

Reference: G. Chen, J. Andries, H. Spliethoff, M. Fang, P.J van de Enden. Biomass gasification integrated with pyrolysis in a circulating fluidized bed. Solar Energy 76 (2004) 345 -349.

The maximum thermal capacity of the CFBG is 100 kW. The fluidizing medium used is air and the average gasifier temperature is 820 °C. The equivalence ratio used for the gasification is 0.3. The gas phase was analyzed by a FT-IR spectrometer; a multi-component gas chromatograph and an online single component analyzer. The composition of producer gas, both in dry and wet compositions are shown in Table 2.7.

**Table 2.7 - Raw producer gas composition for miscanthus pellets**

Gases	Measured (mole fraction)	
	Wet (mol %)	Dry (mol %)
Carbon Monoxide (CO)	10.99	12.57
Carbon dioxide (CO <sub>2</sub> )	14.00	16.02
Methane (CH <sub>4</sub> )	2.14	2.45
Ethene (C <sub>2</sub> H <sub>4</sub> )	0.65	0.74
Hydrogen (H <sub>2</sub> )	5.24	6.00
H <sub>2</sub> O (g)	12.59	0.00
Nitrogen N <sub>2</sub> (calc)	54.38	62.22
LHV (wet, tar free)	3.46 MJ/Nm <sup>3</sup>	
HHV (dry, tar free)	3.69 MJ/Nm <sup>3</sup>	
Tar concentration	75 mg/Nm <sup>3</sup>	

Reference: G. Chen, J. Andries, H. Spliethoff, M. Fang, P.J van de Enden. Biomass gasification integrated with pyrolysis in a circulating fluidized bed. Solar Energy 76 (2004) 345 -349.

From all these compositions for various biomass feedstocks, it can be seen that carbon monoxide, hydrogen and hydrocarbons are the main contributors to the heating value of the fuel. The more the percentage of these quantities, more will the heating value of the fuel and hence increase the thermal efficiency of the gasification process.

## 2.6 Gas clean-up technologies

The syngas or the producer gas produced by the gasification process contains different kinds of contaminants mainly particulates, condensable tars, alkali compounds, hydrogen sulphide (H<sub>2</sub>S), hydrogen chloride (HCl), ammonia (NH<sub>3</sub>) and hydrogen cyanide (HCN). These contaminants can lower the efficiency of producer gas combustion in the burner, when it is used for industrial applications like heating, and also cause potential damage to

the burner. Hence these impurities need to be removed before the syngas or the producer gas could be used for any application. Depending on the type of application, certain impurities are more critical and need to be below a certain limit. Hence there are different cleaning processes depending on the end product desired (Patrick, 2002).

With the current state of the art gas cleaning technology, the contaminants can be eliminated to very low amounts. The gas cleaning usually comprises of dust removal by a cyclone separator, wet scrubbers to cool the gas and remove the tars by condensation and  $\text{NH}_3$  and  $\text{HCl}$  by adsorption, and finally an electrostatic precipitator (ESP) for dust and tar aerosols. A number of experimental results prove that these methods are very efficient in tar removal as well as effective particle capture. Venturi scrubbers have been shown to have an efficiency of 51% - 91%. The tar concentration can go down to as low as 20 – 40  $\text{mg/m}^3$  for a highly efficient scrubber system. It has also been shown that a water scrubber can produce a tar concentration as low as 20 – 40  $\text{mg/m}^3$  and particulate levels of 10 – 20  $\text{mg/m}^3$ . Also wet scrubber is expected to remove about 60% of the tar from the raw gases in a circulating fluidized bed gasifier (Han, 2006).

Another successful method to remove the tar from the raw producer gas is OLGA (oil-based gas washer) technique. Fig 2.2 shows a simplified diagram of the process (Patrick, 2002).

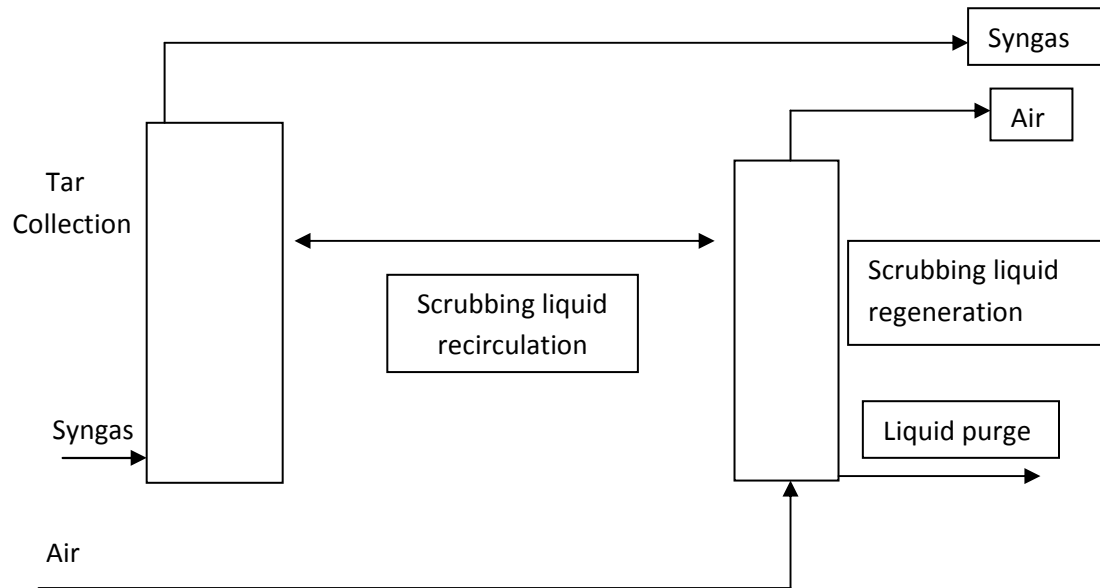


**Fig 2.2 - Schematic of OLGA technique**

The simplified OLGA consists of two scrubbing towers. Syngas is fed to the collector in which the tars are removed to the desired level. The scrubbing liquid with the dissolved tars are regenerated in the stripper. Part of the scrubbing liquid exiting is purged and charged to the gasifier. In case of air blown gasification, air is used to strip the tar.

The main issue with the raw producer gas is the condensation of tar. Hence it is believed that if the dew point of tar is reduced to levels below the lowest expected temperature, fouling related problems by the condensation of tar aerosols are solved. Upstream of the OLGA process, the syngas is cooled and de-dusted. The OLGA process removes the tar impurities from the syngas and then it goes downstream, where non-tar impurities  $\text{NH}_3$  and  $\text{HCl}$  are removed by wet scrubbing and water is condensed out due to further cooling of the gas.

## 2.7 Fate of nitrogen in biomass feedstock

### 2.7.1 Introduction

Nitrogen is a macronutrient in plants that is essential for their growth. Nitrogen in woody biomass is mostly found in the needles and leaves (around 1%), while the bark contains 0.3-0.5% and the wood matter usually contains <0.1% nitrogen. During biomass gasification, the nitrogen in the fuel is released as ammonia, cyanides, molecular nitrogen, nitrogen oxides and various aromatic organic compounds. A very small quantity of this nitrogen is retained in the remaining unreacted solids. The concentration of nitrogen compounds in the product gas depends on the nitrogen content of the feedstock and also the gasification process. It has been found that almost regardless of the gasification process and feedstock used, the predominant compound formed is  $\text{NH}_3$ , while the share of the other nitrogen compounds is small. A study was conducted by the researchers at the Royal Institute of Technology, Sweden to compare the precursors to  $\text{NO}_x$  by measuring the weight percentage of various nitrogen compounds.

For this analysis, five different fuel types were considered. Four of them being solid biomass and other one being coal, to compare the effects of nitrogen distribution in the fuels to the production of different precursors during the gasification process. The gasification process was carried out in a pressurized fluidized bed gasifier.

The gasification process was carried out at 900°C and 0.4 MPa. Oxygen enriched nitrogen was used as the fluidizing agent. The distribution of fuel nitrogen was analyzed in the gases, tar and char resulting from the gasification process, the data for which is provided in the Table 2.8 (Yu, 2007).

**Table 2.8 - Fuel nitrogen distribution in the resultant producer gas**

Raw material	Reed Canary	Miscanthus	Salix	Dawmill coal
% of fuel N in char	0.7	9.4	0.0	34.1
% of fuel N as NH <sub>3</sub>	34.3	12.7	24.4	7.5
% of fuel N as HCN	0.1	0.12	0.22	0.10
% of fuel N as NO	0.20	0.04	0.66	0.10
% of fuel N as NHC	1.30	0.37	0.67	-
Ratio (%) of N(HCN) to	0.29	0.94	0.90	1.33
Ratio (%) of N(NO) to	0.58	0.31	2.70	1.33

Reference: Q-Z Yu, C. Brage, G-X. Chen, K. Sjoström. The fate of fuel-nitrogen during gasification of biomass in a pressurized fluidized bed gasifier. Fuel 86 (2007) 611-618.

Table 2.8 shows that for all the biomass fuels, the majority of fuel NO<sub>x</sub> precursor is ammonia. The fuel nitrogen getting converted to ammonia could be due to three reasons. Firstly, nitrogen in biomass is believed to be mainly in the form of protein and free amino acid. The amine groups are believed to form ammonia directly at relatively low temperatures during pyrolysis. Secondly, the tar from thermo chemical processing of solid fuels will undergo secondary gas phase cracking releasing nitrogen mainly as ammonia. Thirdly, the thermal cracking of char is also an important course for ammonia formation. The presence of ammonia in the producer gas is the main source of NO<sub>x</sub> formation during the combustion of producer gas. Though the amount of ammonia is restricted by the

feedstock used and the gasification process, the formation of NO<sub>x</sub> could be reduced by ensuring relatively low temperatures are used during the combustion of producer gas, preventing the oxidation of molecular nitrogen. This would reduce the thermal NO<sub>x</sub> to good extent. Thermal NO<sub>x</sub> is predominant above temperatures of 1500<sup>0</sup>C. But the nitrogen in the form of ammonia would result in fuel NO<sub>x</sub> formation, which is mainly due to the nitrogen present in the fuel. The characteristics of fuel NO<sub>x</sub> with respect to different conditions of the burner operation are not known clearly and our effort in this work is to understand the behavior of fuel NO<sub>x</sub>.

### 2.7.2 Fuel NO<sub>x</sub> chemistry

Various studies have shown that the main precursor to the formation of NO<sub>x</sub> in biomass is ammonia (NH<sub>3</sub>). The formation of NH<sub>3</sub> requires the presence of the condensed phases of carbonaceous materials rich in hydrogen. Direct hydrogenation of N-sites by the H radicals generated in situ in the pyrolyzing solid is the main source of NH<sub>3</sub> from the solid. The initiation of N- containing hetero-aromatic ring by radical is the first step for the formation of both HCN and NH<sub>3</sub>. While the thermally less stable N- containing structures are responsible for the formation of HCN, the thermally more stable N- containing structures may be hydrogenated slowly by the H-radicals to NH<sub>3</sub> (Li, 2000).

It may be seen that part of the NH<sub>3</sub> observed from the pyrolysis of biomass is due to the presence of amino groups in the biomass. In fact this does not seem to be the main source of NH<sub>3</sub> even from the pyrolysis of biomass. The pyrolysis of amino acids in the solid biomass

would mainly yield HCN. Therefore the direct or indirect hydrogenation of the nitrogen in the hetero-aromatic structures is the main source of  $\text{NH}_3$  from the pyrolyzing solid particles. A simulation study was conducted at the University of Hawaii to understand the behavior of fuel bound nitrogen in biomass feedstocks. The simulation was conducted for fluidized bed gasifiers at an equivalence ratio of 0.25 with oxygen and steam as fluidizing medium, to eliminate the dilution of the nitrogen compounds formed in the gas, with the atmospheric nitrogen due to air blown gasification (Zhou, 1997). The study aimed at understanding the conversion of fuel based nitrogen to different nitrogen compounds like ammonia ( $\text{NH}_3$ ), hydrogen cyanide (HCN), nitric oxide (NO) and diatomic nitrogen. Fig 2.3 shows the conversion of fuel bound nitrogen into different compounds at different gasification temperatures. It is seen that the concentration of ammonia is much higher than that of HCN or NO, and hence can be considered as the single main precursor for fuel  $\text{NO}_x$  formation.

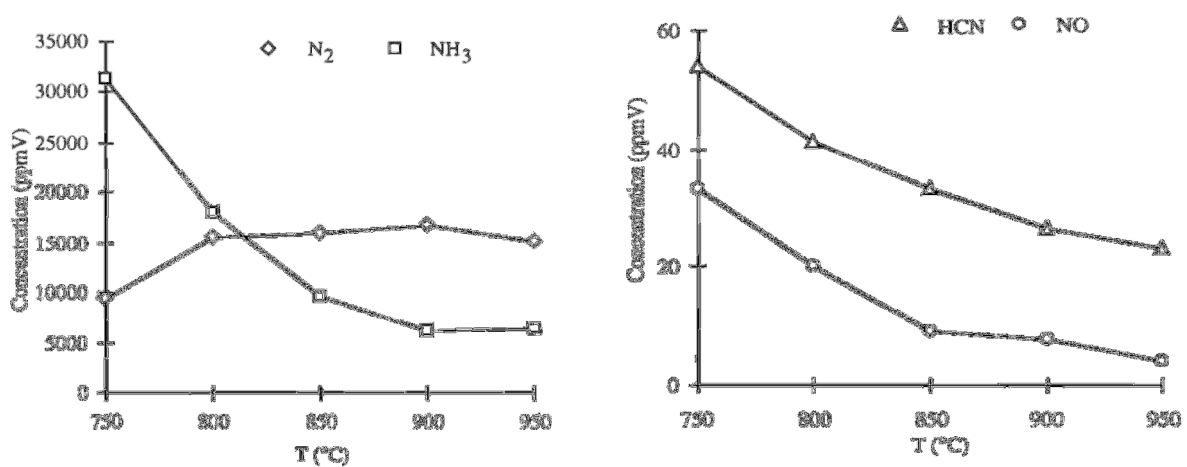


Fig 2.3 Conversion of fuel bound nitrogen in biomass

### 2.7.3 Comparison of thermal NO<sub>x</sub> and fuel NO<sub>x</sub>

The ultimate aim of this project is to reduce the NO<sub>x</sub> emissions from the burner. These NO<sub>x</sub> emissions are mainly due to two reasons. One is the high temperature of combustion, which oxidizes nitrogen compounds and molecular nitrogen (present in air) to nitric oxides (NO<sub>x</sub>). This is called thermal NO<sub>x</sub>, which can mainly be reduced by keeping the temperature of combustion low. The other reason for NO<sub>x</sub> emissions, and possibly the main in producer gas combustion, is the fuel NO<sub>x</sub> produced from the presence of nitrogen compounds in producer gas like ammonia (NH<sub>3</sub>) and HCN. The third way NO<sub>x</sub> formation occurs is by the prompt NO<sub>x</sub>. Prompt NO<sub>x</sub> is formed during the early, low temperature states of combustion and is insignificant.

Thermal NO<sub>x</sub> is mainly caused due to high flame temperatures during the combustion process. The main aim is to reduce the thermal NO<sub>x</sub>, which can be achieved by reducing the flame temperature. In recent years, lean premixed (LPM) combustion has been used to reduce pollutant emissions by controlling the flame temperature. Lower flame temperatures in LPM combustion reduce soot and thermal nitric oxide production, although unburned hydrocarbon (UHC) and carbon monoxide (CO) emissions rise as the lean blow-off (LBO) limit is reached. Thus the flame temperature in the combustor must be sufficiently high to prevent the LBO and to minimize emissions (Alavandi, 2008).

One of the major concerns in the combustion of producer gas is the production of fuel NO<sub>x</sub>. The main precursors of fuel NO<sub>x</sub> during the biomass gasification are NH<sub>3</sub> and HCN. In

biomass, nitrogen mainly exists as proteins and amino acids, together with some other forms such as DNA, RNA, alkoids, porphyrin, and chlorophyll. The thermal cracking of volatiles is seen to be one of the main routes of  $\text{NH}_3$  formation during the pyrolysis of biomass. During gasification, the distribution of fuel-N into volatile-N and char-N is significantly dependent on fuel rank. A large fraction of biomass-N would become volatile-N, which under gasification conditions in the presence of gasifying agents like steam could reform, leading to the formation of HCN and  $\text{NH}_3$  (Tian, 2007).

Experiments were conducted on a set of fuels ranging from cane trash to sewage sludge and the formation of HCN and  $\text{NH}_3$  were reported. Fig 2.4 below shows the reaction time resolved accumulated yields of  $\text{NH}_3$  during the gasification of cane trash. The first points in these figures refer to the yields from the feeding periods, during which biomass particles were continuously fed into the reactor. The other points refer to the yields from the “not feeding” periods, in which the feeding of biomass had stopped and the char inside the reactor continued to be gasified.

During the gasification of cane trash, majority of  $\text{NH}_3$  was formed in the feeding periods. There are two pathways to form  $\text{NH}_3$ : the hydrogenation of char-N by H radicals or the thermal cracking of volatile-N in the gas phase. Due to the presence of frit in the freeboard of the one stage fluidized bed reactor, there would be strong interaction between the volatiles and char. The volatiles generated within the fluidized bed contain H-rich structures and would readily be thermally cracked to generate radicals. As the radical rich

volatiles passed through the frit, the H radicals would react with the nascent char held underneath the frit to form  $\text{NH}_3$ .

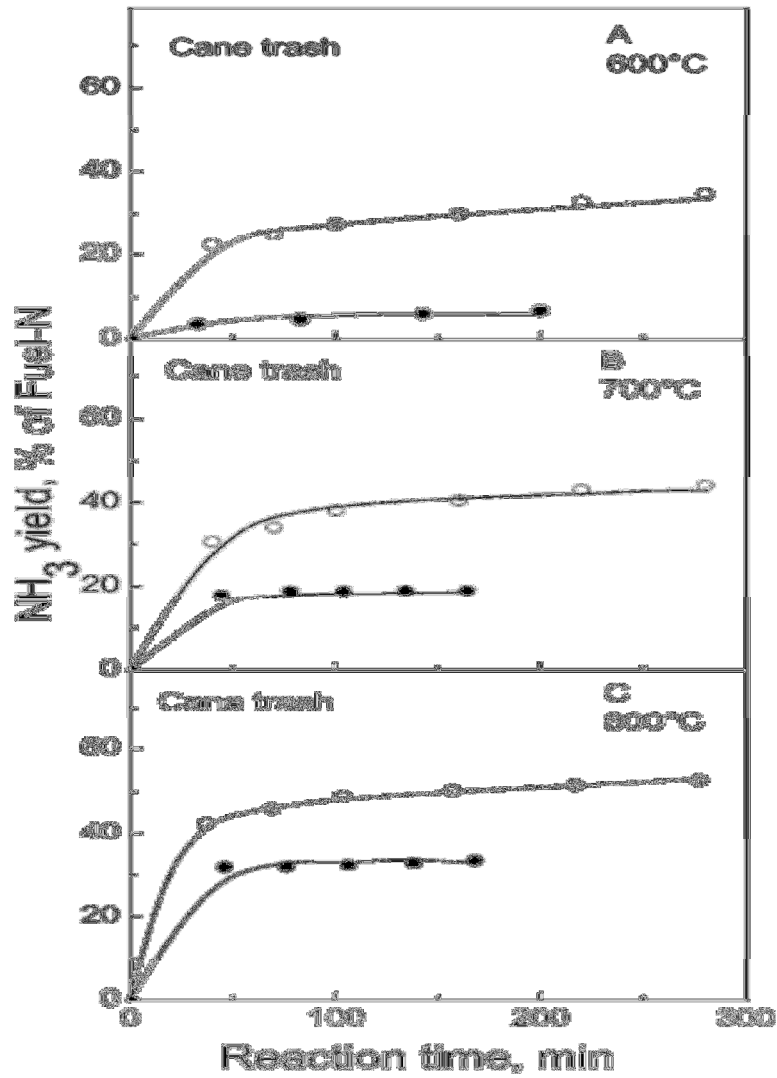


Fig 2.4 - Ammonia formation at different gasification temperatures for cane trash

## 2.8 Producer gas combustion

### 2.8.1 Differences between syngas and producer gas

Synthesis gas (syngas) and producer gas are both obtained from the gasification process, but they differ in their compositions and other characteristics. The dominant species in the syngas include hydrogen ( $H_2$ ) and carbon monoxide (CO), usually in the ratio of 1:2. Producer gas, which typically has a lower energy content than the syngas, also contains traces of ethane, ethylene, propane and other hydrocarbons, along with ammonia, hydrogen sulphide. Syngas is usually a product of high temperature gasification process, particularly using coal. In a high temperature gasification environment, the higher hydrocarbons are converted to CO and  $H_2$ , thus increasing the heat content of the gas mixture. Producer gas is a product of low temperature gasification (particularly using biomass) and hence most of the hydrocarbons do not get oxidized. Air gasification of biomass feedstock generally results in producer gas, because of low temperatures of gasification as a result of dilution of the fluidizing medium with atmospheric nitrogen, which does not take part in the reactions. Oxygen and steam blown gasification result in high gasification temperatures and hence leads to the formation of syngas with higher energy content. The producer gas needs to be cleaned to remove impurities like tar, particles and other trace chemical elements before entering the burner. The heating value of producer gas is low, typically around 5.5-7.5 MJ/Nm<sup>3</sup>, approximately 15-20% of the heating value of natural gas (Wang, 2007).

## 2.8.2 Status of producer gas combustion research

The most important aspect when analyzing the combustion properties of any gas is to examine the ignition properties and the flame propagation characteristics. Since producer gas mainly contains carbon monoxide (CO) and hydrogen (H<sub>2</sub>), the combustion property of producer gas would be directly influenced by the properties of CO and H<sub>2</sub>. Studies have been conducted to understand the auto-ignition characteristics of H<sub>2</sub>/CO mixtures. The following study was carried out in a rapid compression machine (RCM) at compressed pressures (P<sub>c</sub>).

Sung (2008) has conducted studies to measure the laminar flame speeds for CO/H<sub>2</sub>/air as a function of equivalence ratio with different fuel concentrations and mixing ratios for pressures of 1, 2, 5, 10, 20, and 40 atm, with comparison to measured data from literature and also calculated values from different mechanisms. It is seen that the measured flame speeds increase with increasing H<sub>2</sub> content in the CO/H<sub>2</sub> mixtures. Fig 2.5 shows the plots of laminar flame speed at different equivalence ratios for pressures of 1 and 2 atm. Different ratios of CO and H<sub>2</sub> are analyzed to see the effect of adding or removing CO and H<sub>2</sub>. It is seen that the addition of H<sub>2</sub> increases the overall laminar flame speed of the mixture. H<sub>2</sub> has the highest laminar flame speed, with hydrocarbons having a value close to that of H<sub>2</sub>. High flame-speed combustion processes, which closely approximate constant-volume processes, should result in high efficiencies.

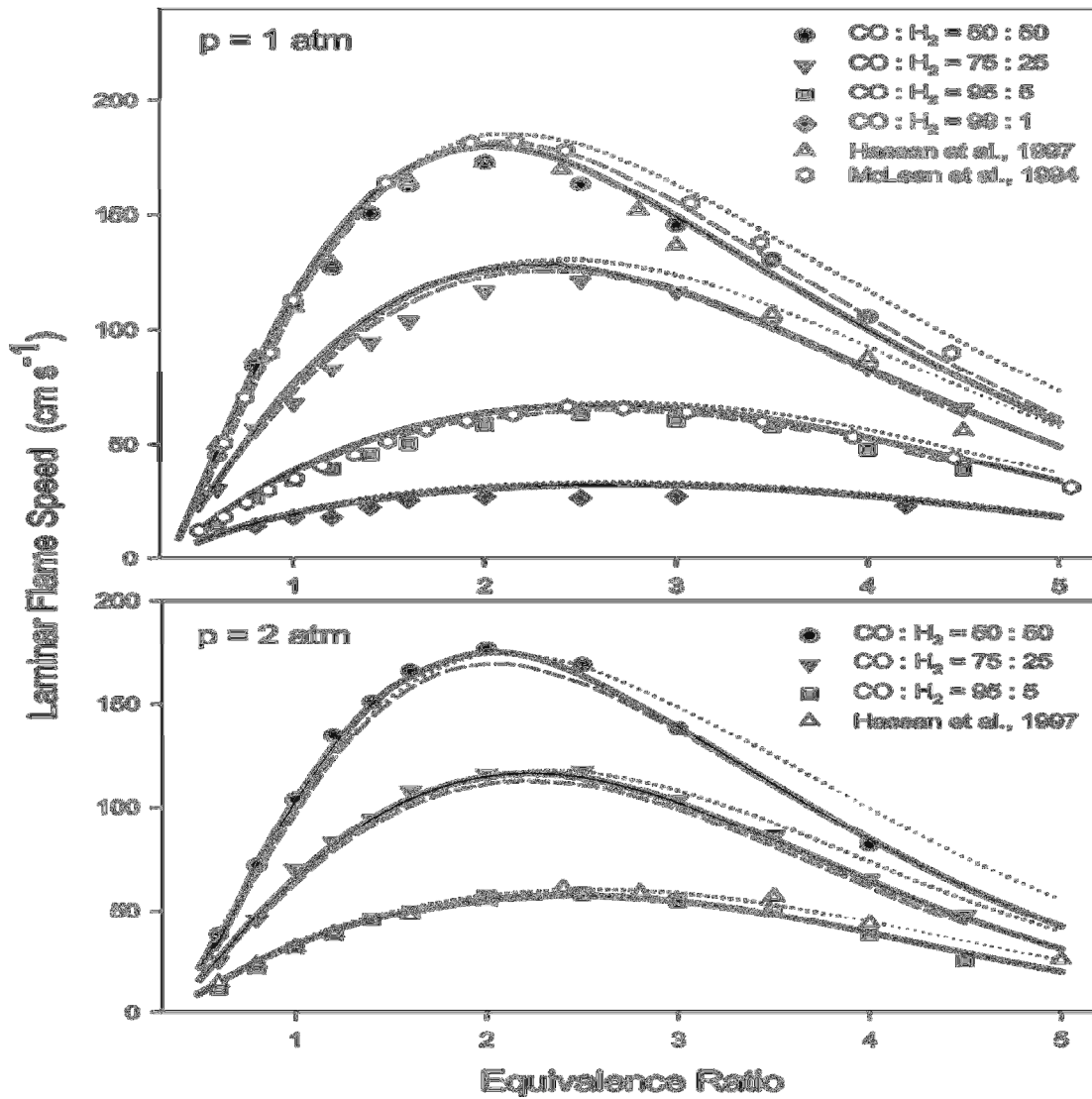


Fig 2.5 - Laminar flame speed for CO/H<sub>2</sub> mixtures at different pressures

Despite the recent technological advances, the experimental measurements of laminar flame speed, extinction limits, and ignition limits over a wide range of syngas compositions and initial conditions are still needed.

A study was also conducted to investigate lean premixed combustion of hydrogen-syngas/methane experimentally to demonstrate the fuel flexibility of a two-section porous

burner. Lower temperatures in lean premixed combustion reduces soot and thermal nitric oxide production, although unburned hydrocarbon and carbon monoxide emissions rise as the lean blow-off limit is reached. Results show CO emissions decreasing with increasing amounts of H<sub>2</sub>/CO in the fuel mixture. The NO<sub>x</sub> emissions are virtually unaffected by the fuel composition, evidently because of the insignificant thermal NO<sub>x</sub> produced at lower temperatures (Alavandi, 2008).

Experiments were conducted by the University of Alabama to investigate the effect of adiabatic flame temperature on CO and NO<sub>x</sub> emissions for different concentrations of CO, H<sub>2</sub> and CH<sub>4</sub>, the trend of which is shown in Fig 2.6. The temperature operating range of fuels with H<sub>2</sub>/CO is different from that of CH<sub>4</sub> because of the constraints imposed by the flame flashback and lean blow off limit. In fuels with H<sub>2</sub>/CO, the flame is sustained at lower temperatures, evidently because of the high reactivity of H<sub>2</sub>. However at these low temperatures, the CO oxidation reactions are slower, and hence higher CO emissions are produced. Since the combustion properties of producer gas are mainly dictated by the combustion characteristics of CO and H<sub>2</sub>, these results are essential in understanding the combustion of producer gas.

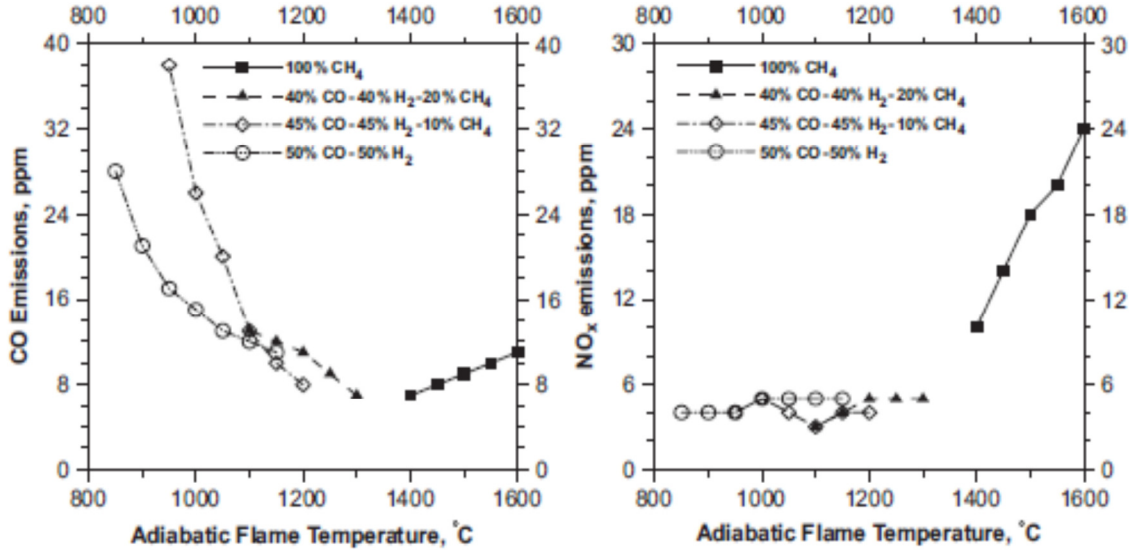
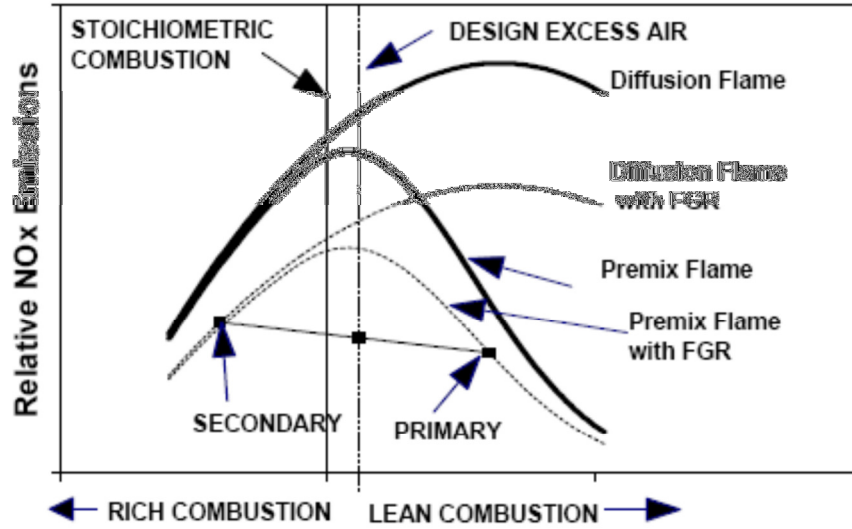


Fig 2.6 - Effect of adiabatic flame temperature on CO and NO<sub>x</sub> emissions

### 2.8.3 Low BTU Burner

There are different techniques that have been applied to reduce the NO<sub>x</sub> emissions from the burners. The techniques that are most often used are utilization of air staging, fuel staging, flue gas recirculation and combinations of these to meet the required emission level.

The flame stoichiometry for a burner has been studied with four different types of flames in a research conducted by John Zink. These flames are non-premixed diffusion flame and premixed flame, without flue gas recirculation and with flue gas recirculation. Fig 2.7 below shows the comparison of NO<sub>x</sub> emissions for these different flames (Athens, 1995).



**Fig 2.7 - NOx emissions for different flames with and without FGR**

The curve shows that the NOx emissions are depressed for either premix or diffusion flames under fuel rich or sub-stoichiometric conditions with flue gas recirculation and also for very lean premixed flames with flue gas recirculation. It can be observed from the figure that operating with more than one combustion zone can lead to very low NOx emissions with reasonable overall excess air in the final combustion products. It is seen that firing a part of the fuel as a lean premix flame with flue gas recirculation will produce low NOx in that combustion zone. Firing the remaining fuel under fuel rich conditions with flue gas recirculation will produce low NOx emissions in the other combustion zone. Then properly combining the lean and rich combustion products to form a final burnout zone ultimately allows operation with low excess air and very low NOx emissions. Hence a two stage combustion process is most often the preferred technique for the production of low NOx exhaust in the operation of a burner.

The three ways in which NO<sub>x</sub> could be formed are thermal NO<sub>x</sub>, fuel NO<sub>x</sub> and prompt NO<sub>x</sub>. Thermal NO<sub>x</sub> is mainly formed at high temperatures of combustion, and the main contributor to its formation is the nitrogen from the air. Fuel NO<sub>x</sub> is formed from the nitrogen compounds present in the fuel like NH<sub>3</sub> and HCN. Prompt NO<sub>x</sub> is mainly formed due to the presence of hydrocarbons. The nitrogen from the air combines with the hydrocarbon radical to form the precursors of prompt NO<sub>x</sub>.

A schematic of the common process used in a low NO<sub>x</sub> burner is given below in Fig 2.8 (Yamagishi, 1975).



**Fig 2.8 - Schematic representation of low NO<sub>x</sub> burner process**

A study was also conducted by the Department of Chemical Engineering, Brigham Young University, Utah to validate the impact of fuel type (biomass and coal) on the generation of nitrogen species by mapping species like NH<sub>3</sub>, HCN, CO, CO<sub>2</sub> etc in a low NO<sub>x</sub> burning environment. CO and CO<sub>2</sub> were used to conclude whether it was a fuel rich or a lean combustion zone. It was found that NH<sub>3</sub> was the main precursor to the formation of NO<sub>x</sub> in biomass.

## CHAPTER 3: METHODS AND PROCEDURES

### 3.1 Introduction

This chapter summarizes the gasification system, the combustion system and the measurement techniques used to carry out this study. Each section outlines the capacities of different systems, limitations of different techniques and methods used to conduct the experiments.

### 3.2 BECON gasification system

A pilot-scale gasification system at the Bio-energy conversion (BECON) facility in Nevada, IA was used to conduct the experiments. The gasification setup was operated by Frontline Bioenergy, LLC. The system consists of a feeding auger, a pressurized vessel, a fluidized bed reactor, and various gas clean-up components. The system is rated at 800 kW thermal input, corresponding to a feeding rate of 180 kg/hr of solid biomass with a heating value of 16,000 kJ/kg. The gasifier was operated under fuel-rich conditions at an equivalence ratio varying between 0.22 and 0.25. Note that the equivalence ratio here is defined as the ratio of the actual air-fuel ratio to the stoichiometric air-fuel ratio. This definition is the inverse of the traditional definition used in combustion applications. The present definition is consistent with that used in the gasification industry.

The bubbling fluidized bed gasifier at Becon is shown in Fig 3.1. Solid biomass is pelletized and fed to a vessel at atmospheric pressure using a feed auger. The cylindrical biomass pellet is approximately 15 mm in length and 5 mm in diameter. The feeding mechanism is

screw operated, which feeds the biomass feedstock into the vessel at a constant rate as shown in Fig 3.2. Once the vessel is filled to its capacity, this vessel is pressurized to about 15 – 18 psi gage pressure and the feedstock is transferred to another pressurized vessel, also maintained at the same pressure. Air is purged into the first vessel to prevent the backflow of producer gas. The feedstock is then introduced into the bubbling fluidized bed reactor, which is air blown from the bottom. The fluidized bed has a bed depth of 1 – 1.3 m and is operated under atmospheric pressure conditions. The temperature inside the gasifier is maintained at 815 °C to attain steady-state conditions by using electrical heating coils. Limestone is used to prevent bed agglomeration and reduce the tar formation.



**Fig 3.1 - Bubbling fluidized bed gasifier at BECON**

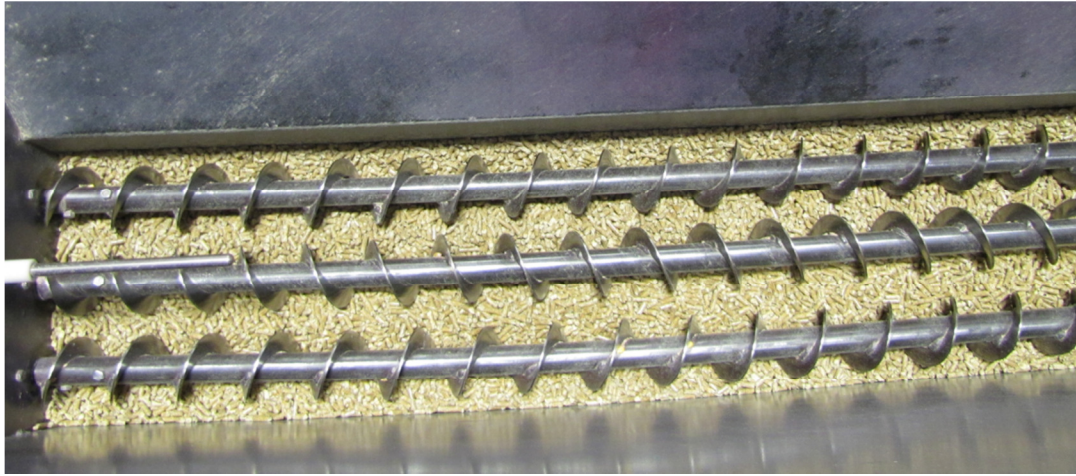


**Fig 3.2 - Feed auger with screw operated mechanism**

Biomass feedstock at such elevated temperature conditions with insufficient oxygen will be gasified to form producer gas, containing carbon monoxide (CO), hydrogen (H<sub>2</sub>), nitrogen (N<sub>2</sub>), methane (CH<sub>4</sub>) along with other hydrocarbons, ammonia, water, char, and tar. The gas coming out of the gasifier is at a pressure of 15 – 18 psi gage. The producer gas contains a lot of impurities in the form of char, tar and sulphur compounds, which restricts the application of producer gas as a source of energy. The impurities in the form of heavy char particles need to be removed before the gas is sent to the burner for combustion. During the gas cleaning stage (i.e., gas conditioning), the gas from the fluidized bed reactor is passed through a baghouse to remove the char particles and ash in order to prevent the pipes from clogging over time. The baghouse is essentially a cyclone filter, which separates heavy char and ash particles by gravimetric method, a picture of which is shown in Fig 3.3. The gas coming out of the baghouse is usually at 5 psi gage and a temperature of 400 °C. The schematic representation of the entire gasification system is shown in Fig 3.4.



**Fig 3.3 - Char collected at the bottom of baghouse**

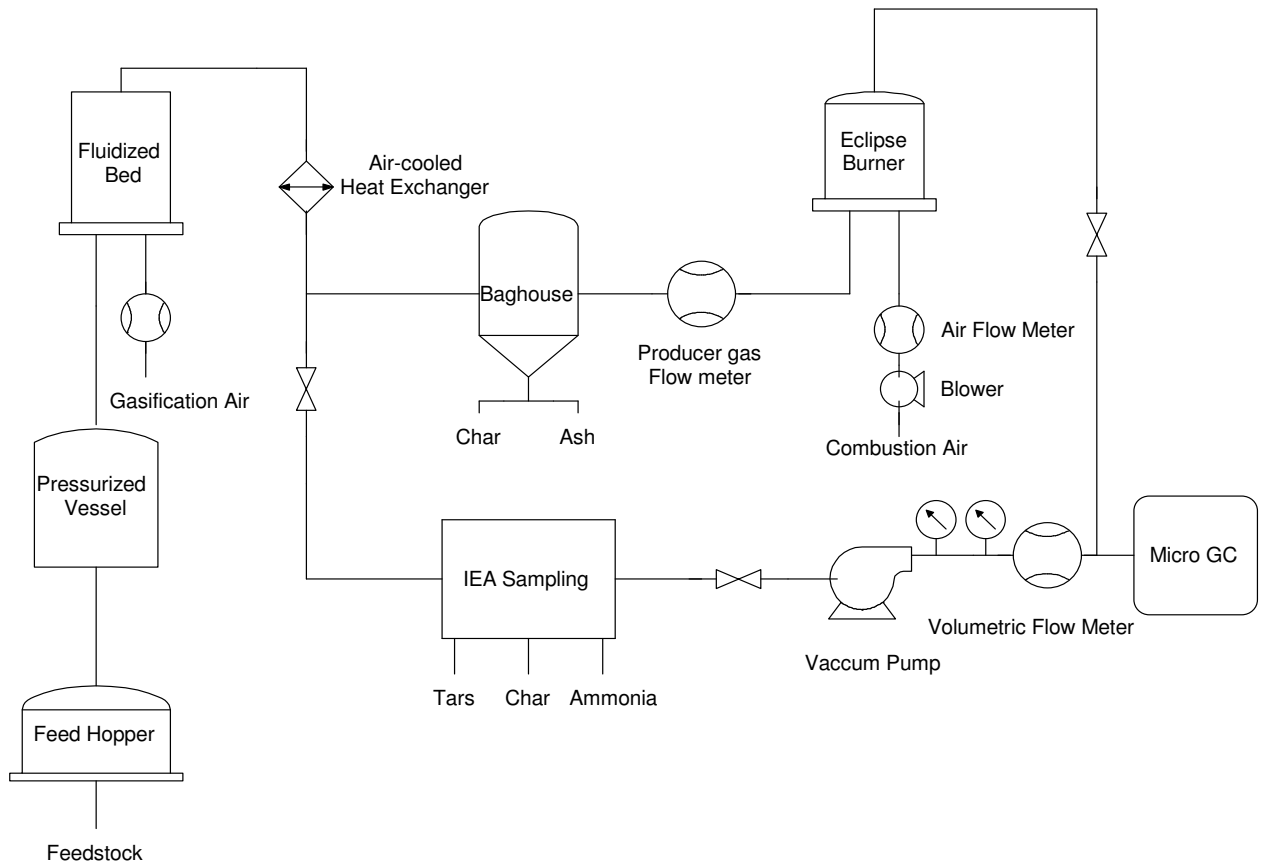


**Fig 3.4 - Schematic representation of the gasification and the combustion system**

### 3.3 COMBUSTION SYSTEM

An industrial burner was used for producer gas combustion. The burner is Eclipse TJ-0300, a medium velocity burner. It is rated at a maximum input of 879 kW. The producer gas coming out of the baghouse flows through a gas flow meter which measures the flow rate of the gas before entering the non-premixed burner. This producer gas is at a high temperature ( $325^{\circ}\text{C}$ ) when entering the burner, thus it is unsafe to operate in the premixed mode to prevent explosion in the fuel-air inlet.

The flow meter is an orifice plate flow meter that has been calibrated for measuring the high temperature producer gas. A combustion chamber surrounds the burner to prevent heat loss to the surroundings and to carry away the exhaust gases. The combustion chamber is built with refractory lining in order to reduce heat loss. The combustion chamber also ensures that the flame is stable without external disturbances. The combustion chamber is shown in Fig 3.5. Producer gas enters the burner through the bottom inlet. The entry of fuel and air are shown in Fig 3.6. The atmospheric air is blown by a motor and enters the burner in four different stages. In the first three stages, the air is introduced through a series of holes that are located at different positions. In the fourth stage, the air enters the exit of the burner. The first three stages create rich mixtures and the fourth stage is to create lean mixtures in order to oxidize any unburned hydrocarbons. The burner is initially fired up using natural gas and then slowly switched to use producer gas. The flame length is usually around 1 m from the base of the burner and varies with biomass feedstock and equivalence ratios. Thermocouples are placed at different heights along the axis of the combustion chamber to obtain an overall idea of the temperature distribution inside the chamber. Since producer gas is a low heating value fuel as compared to natural gas, higher fuel flow rates are needed to maintain the same heat rate and also to provide a stable flame. The exhaust gas sample passes through a set of impingers placed in an ice bath to remove the moisture in the gas. The dry flue gas is then analyzed for its composition.



**Fig 3.5 - Combustion chamber surrounding the burner**



**Fig 3.6 - Point of entry for fuel and air**

### **3.4 Producer gas analysis**

#### **3.4.1 Micro gas chromatograph (GC)**

Producer gas and combustion exhaust flue gas are analyzed using a micro gas chromatograph (GC), which measures the dry gas composition. The micro GC is a Varian CP-4900 Quad Micro GC that has four columns. It works on the principle of comparing the thermal conductivities of various gases with reference to carrier gases such as Helium and Argon. Depending on the thermal conductivities, different gases elute at different times. Since water is removed from the producer gas before it is analyzed by the micro GC, ammonia, being soluble in water is also removed from the producer gas. Therefore, to

analyze ammonia and tar in the producer gas, the International Energy Agency (IEA) tar protocol was followed (Good, Ventress et al. 2005).

### **3.4.2 International Energy Agency (IEA) tar protocol**

This guideline provides a procedure for the sampling and further analysis of tars and particles in biomass derived producer gas. It is valid for updraft and downdraft fixed bed gasifiers and also for fluidized bed gasifiers. In fluidized bed gasifiers, raw producer gas contains concentrations of tars in the order of approximately 20 g/Nm<sup>3</sup> (Knoef, 1999). The motivation for further research on tar quantity and consistency is given not only by the technical issues in the producer gas transportation, storage, and use, but also in the toxicity of these compounds to human health and environment in general.

The sampling line described by the guideline consists of four modules including a module for gas preconditioning in which the sample is obtained and conditioned to a certain temperature and pressure, some sort of filter or device for particle separation and collection, the tar collection module, and last but not least the volume sampling with included temperature and pressure measurement and recording as shown in Figure 3.7.

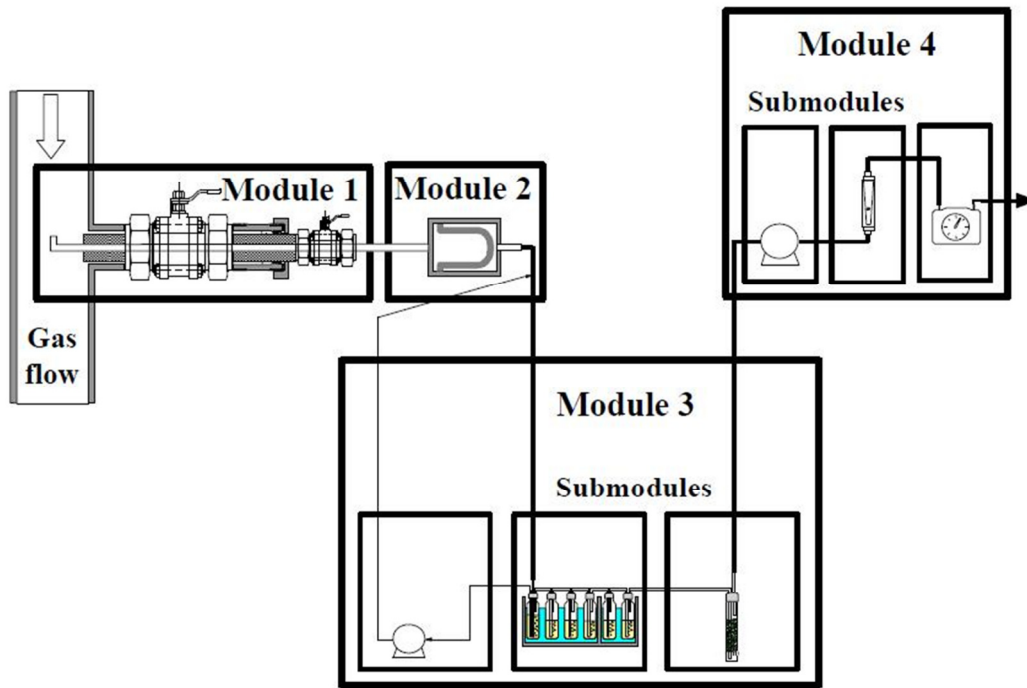


**Fig 3.7 - Scheme of the sampling line for the IEA Tar Protocol**

The IEA protocol is based on the principle of discontinuous sampling of a gas stream containing particles and tars under iso-kinetic conditions. First the sample is drawn from the producer gas pipe with a heated probe. This module is responsible for the preconditioning of the sample gas. The pressure is adjusted, and depending on the gasifier type, the gas is either heated or cooled. In the second module, all the solid components in the sample gas stream are separated from the gas and collected for further analysis. These particles consist mainly of carbon particulates, called char, but depending on the feed stock, heavy metal contents can be found in these chars. The third module is an impinger train with six impinger bottles shown in Fig 3.7. The setup for collecting tars consists of a set of six impingers. Among these six impingers, three are placed in a water bath maintained at

40 °C and the other three are maintained at – 20 °C. The low temperature of – 20 °C is maintained with the help of a mixture of salt, water and ice. Since tars usually drop out at 80 °C, the higher temperature bath (40 °C) ensures the smooth condensation of the tar in order to prevent clogging. The first impinger consists of 100 ml of isopropyl alcohol (IPA), the next four contain 50 ml of IPA, and the last impinger is left empty. Since the temperatures are low, water vapor must condense in these impingers. Since ammonia readily dissolves in water, condensed water would contain ammonia in it, and these are collected in all the six impingers. Hence these six impingers should contain all of tar, with some quantity of water and ammonia.

The gas coming out of the six impingers would contain little bit of moisture along with ammonia. Hence an additional set of three impingers containing distilled water and 0.05% HCl solution is placed downstream of the above six impingers to collect any ammonia that might have slipped from the six impingers in the form of ammonium chloride ( $\text{NH}_4\text{Cl}$ ) and ammonium hydroxide ( $\text{NH}_4\text{OH}$ ). This is a safety measure to make sure all the ammonia is captured. A sufficient sampling time is allowed to pass around 10 cu. ft. of producer gas through these impingers. This usually corresponds to a sampling time of two hours. The IEA setup along with the three impingers downstream is shown in Fig 3.8.

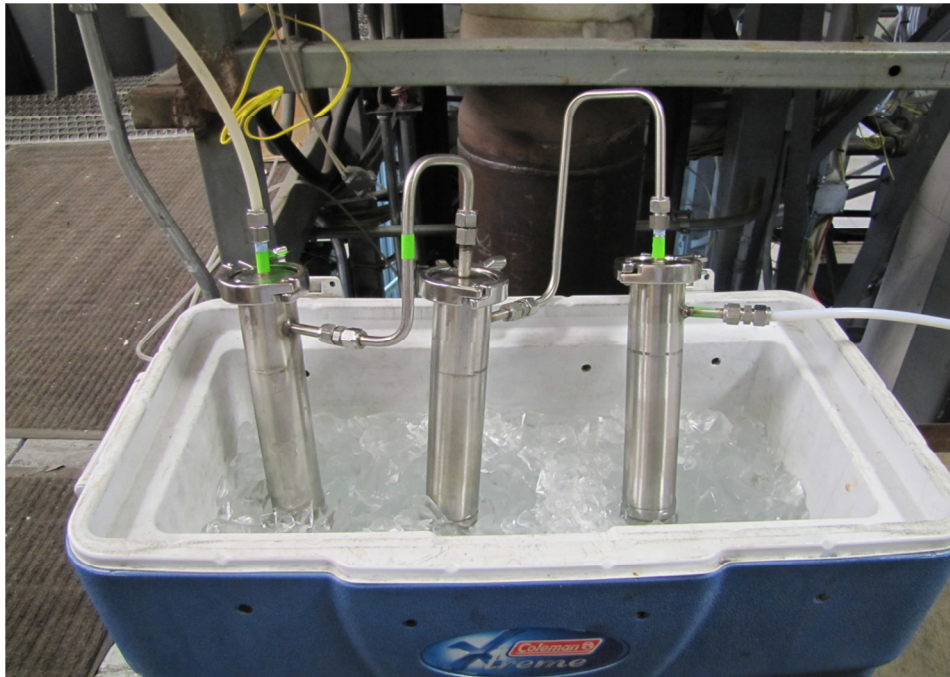
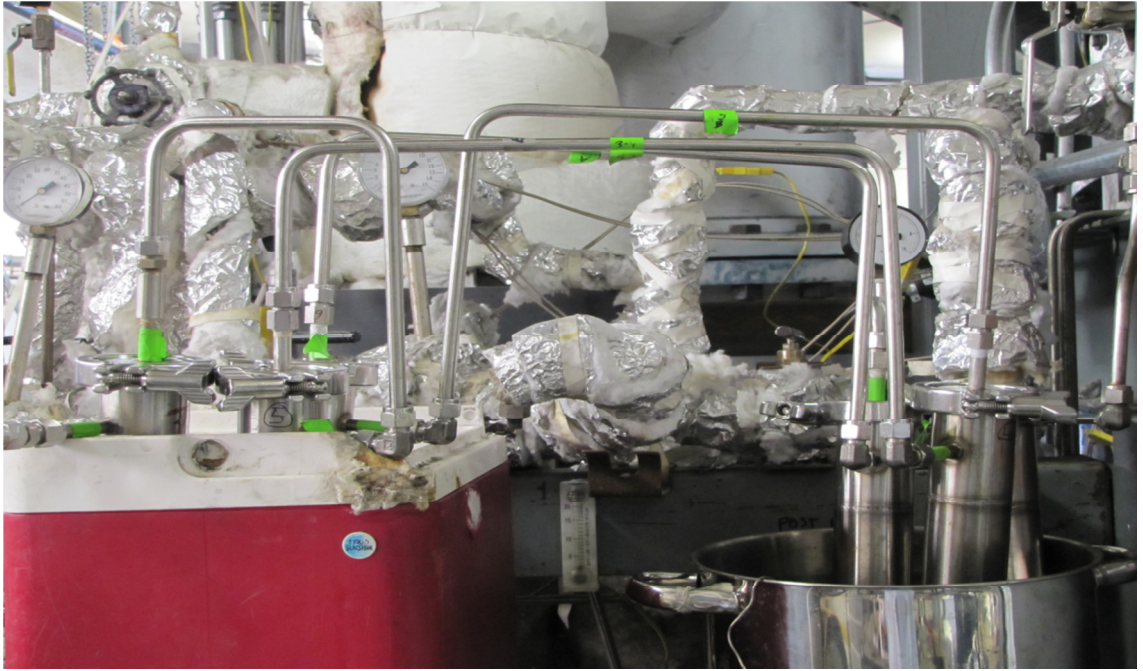


Fig 3.8 - IEA setup with the three impingers downstream

After the sample is collected, the sample valve is closed, and the contents in the impingers are allowed to cool to release any unwanted pressure in the impingers. Sufficient precaution must be taken to ensure that the sample in the impingers are brought to room temperature before collecting them, else it would result in loss of sample. The sample from the impinger is then carefully transferred into PTFE bottles, and these samples are stored at temperatures of 5 °C or below. The samples from the impingers 1 to 6 are collected into two bottles named primary and rinse respectively. The primary mainly contains all the contents of impingers 1 to 6 that are easily transferrable. There are tars and salts that remain stuck to the impingers and are difficult to collect. Reagents like IPA, di-chloro methane (DCM) are used to separate the tars, and water is used to separate the salts from the impingers. This solution is collected in the rinse.

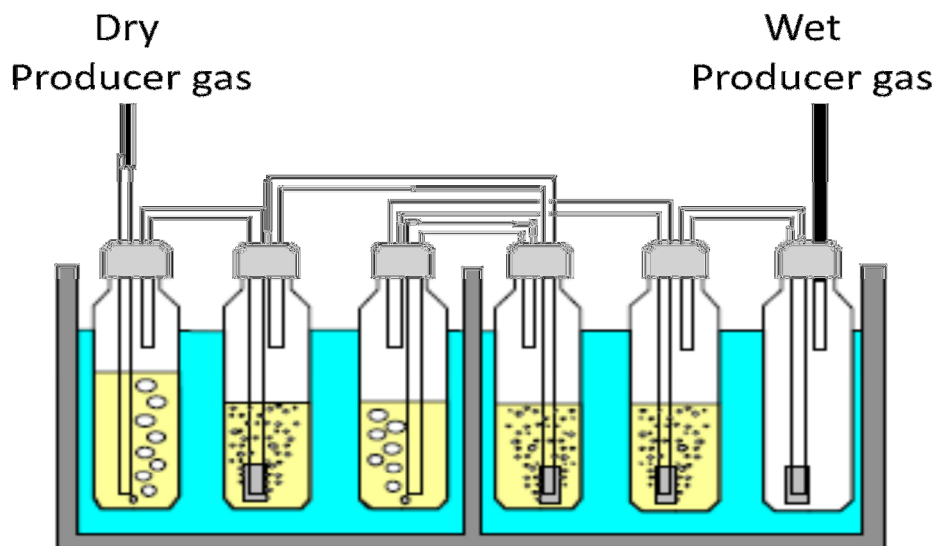
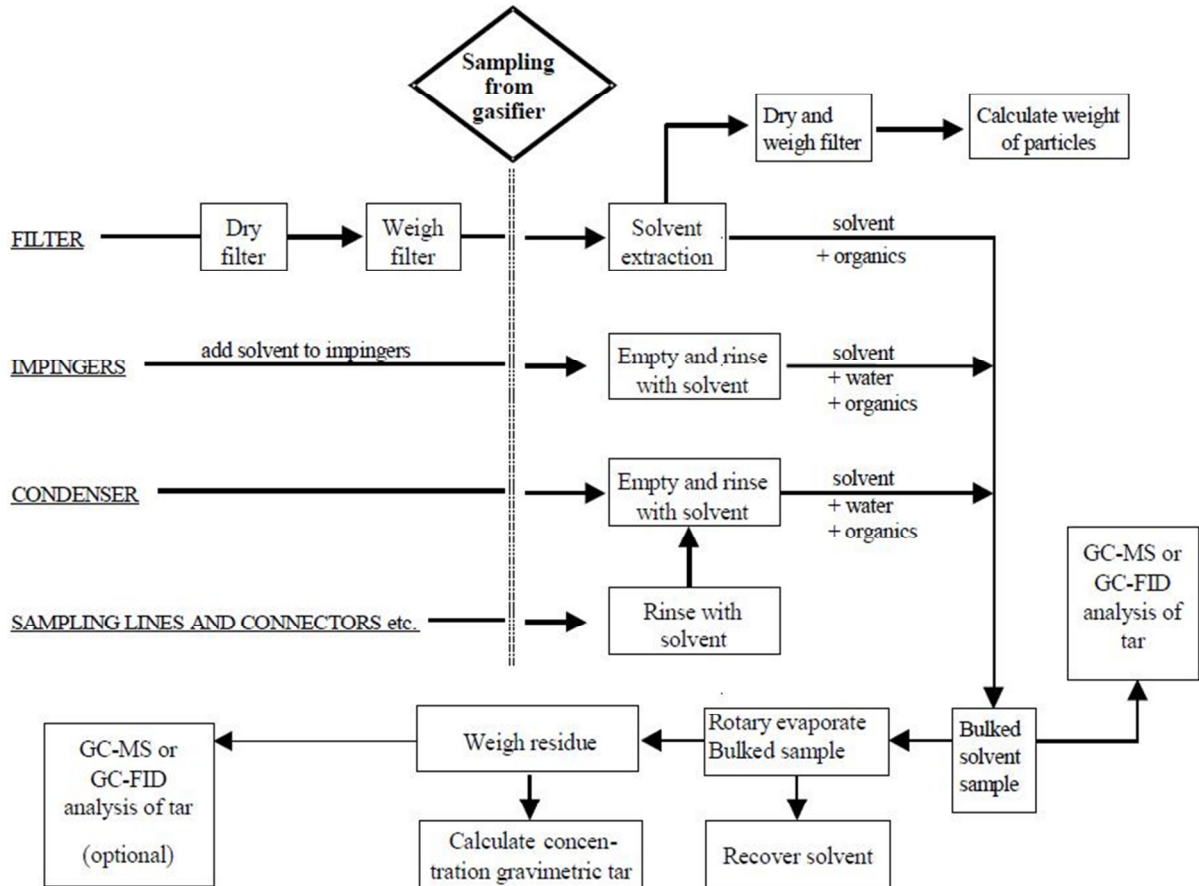


Fig 3.9 - IEA sampling method

Figure 3.10 shows a simplified representation of the sampling and analysis procedure and chronology.



**Fig 3.10 - Sampling and analysis Procedure**

To calculate all the collected compounds back to the actual concentrations in the producer gas, the gas flow properties such as volume, temperature, and pressure are measured and recorded in the fourth module. A dry gas meter with a thermocouple and pressure gauge provided the needed data.

### 3.4.3 Moisture analysis

Since the micro GC gives the dry gas composition, to obtain the actual gas composition of the producer gas, i.e., the wet gas composition, the amount of water vapor in the producer gas needs to be determined. A Karl Fischer titrator was used to measure the moisture content from the sample collected in the impingers. The sample in the primary bottle is used to determine the moisture content as it contains the undiluted sample. The Karl Fischer titrator gives the weight percentage of water in a given sample. The instrument is checked for few specific concentrations of water, close to the range that is expected from these samples. The deviation of the actual value from the measured value is corrected for in the final calculation of moisture from the actual sample. The moisture content obtained in the sample is then correlated to the amount of moisture in the producer gas by measuring the volume of gas passing through the impingers.

### 3.4.4 Tar and ammonia separation

Tar found in biomass-derived producer gas is a complex material consisting of hundreds of different compounds that vary widely in polarity and molecular weight, ranging from 80 g/mol to more than 300 g/mol. The analysis of the collected samples should be completed no more than one month after the collection of the sample even when stored under proper conditions in a dark PTFE bottle.

The collected sample from the impingers mainly contains tar, char, and salts dissolved in water. The collected solution from the impingers is then roto-evaporated to separate out all the distillates like IPA, DCM from the tar. The equipment consisting of the roto-

evaporating unit and a chiller unit is shown in Fig 3.11. The roto-evaporating unit consists of six flasks into which the solutions from the primary and rinse are equally distributed. Since tar has a boiling point of 80 °C and above, the sample is gradually heated from room temperature to around 60 °C to remove all the distillates such as IPA, DCM, acetone, and other hydrocarbons used as solvents. The flasks revolve, subjecting the contents in them in a swirling motion. This allows for uniform heat distribution. The sample may also contain water, which, if in large quantities, would take a long time to be separated from tar, with the sample being heated to a maximum temperature of 60 °C. Hence, methanol is added to water to accelerate the evaporation of water and help with the complete separation of water from tar. The chiller has a vacuum pump in it to accelerate the evaporation process. The flask in the chiller collects all the distillates, which come from the roto-evaporating unit. The outlet of the chiller is connected to a set of three impingers containing distilled water. These impingers ensure the entrapment of ammonia that may otherwise escape in the vapor phase. The tar collected as shown in Fig 3.12 can be characterized in a gas chromatography with flame ionization detection (GC-FID). This process of distillation usually takes about 2-3 hours, depending on the quantity of water in the mixture.



**Fig 3.11 - Roto evap system with a chiller (left) and the samples equally distributed in six flasks (right)**

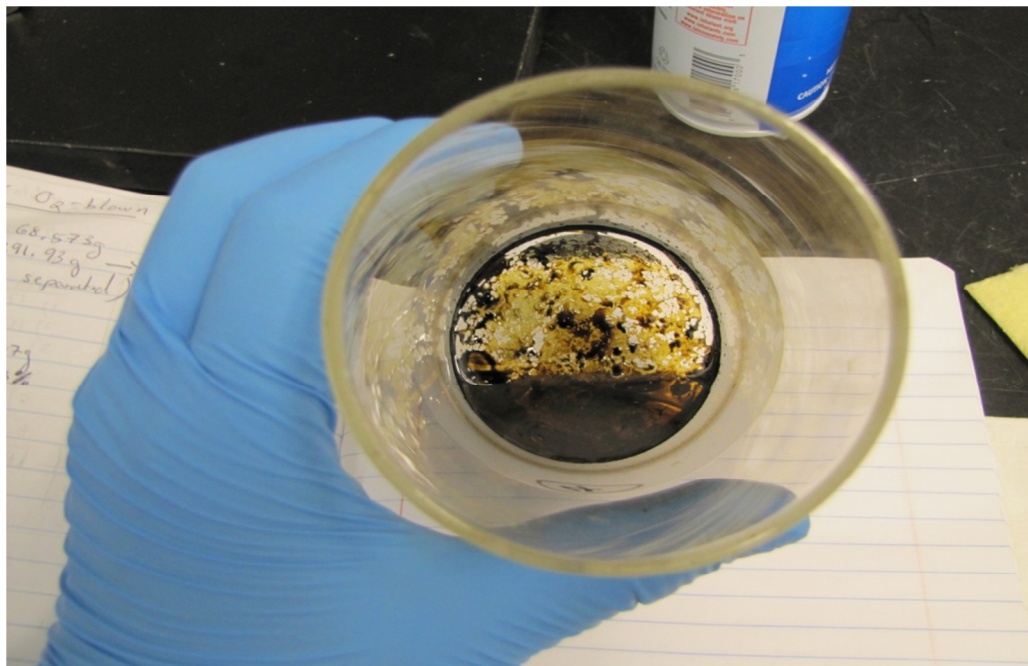


**Fig 3.12 - Tars after the distillation process.**

### 3.4.5 Ammonia analysis

The samples from the distillate and the three impingers downstream used in the tar and ammonia separation process are collected in PTFE bottles, so that they can be analyzed for ammonia using an Aquanal ammonium test kit. After adding the reagents to the sample for the ammonia analysis, the sample is placed in a UV-visible spectrophotometer, which gives the intensity of the light at a wavelength that corresponds to the color of the ammonium ions in the visible range. This intensity, in terms of absorbance, is then correlated to the calibration curve to obtain the exact ammonia content in the sample. The calibration curve co-relates the ammonium ion concentration in mg/L to the absorbance (AU) as shown in the graph in Fig 3.13. The ammonia content in the producer gas is then calculated using the known ammonia concentration in the analyzed samples.

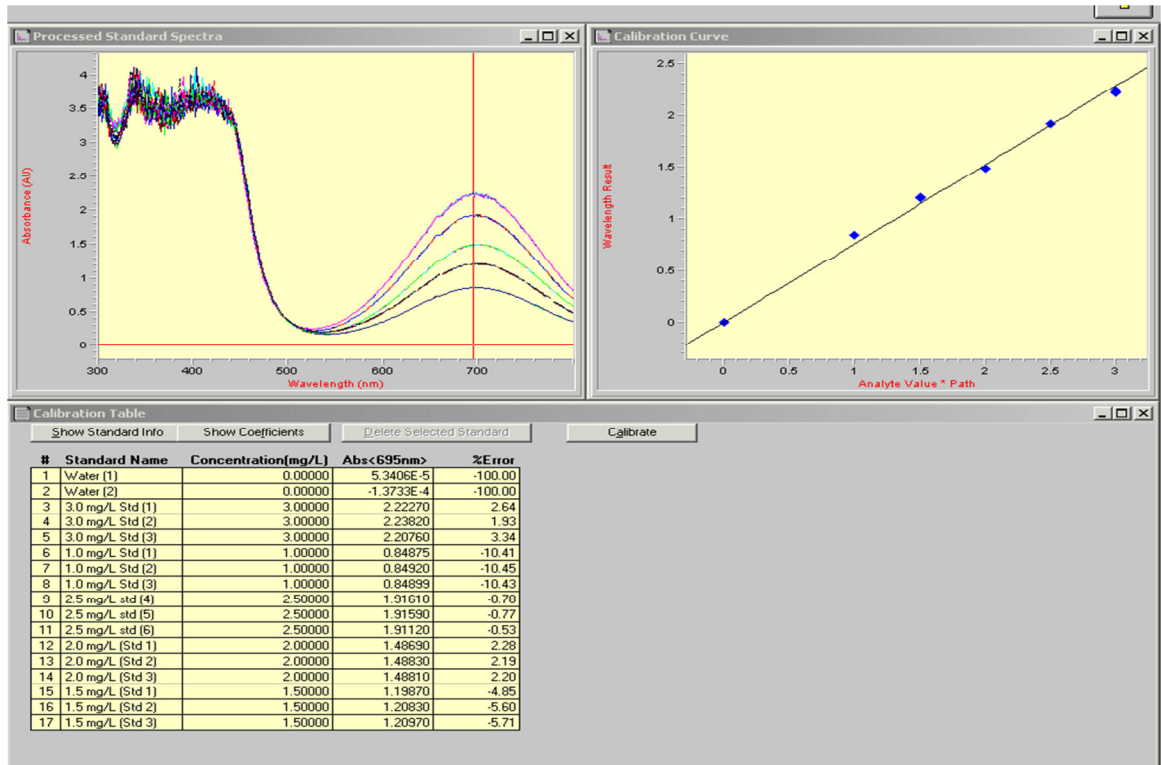


Fig 3.13 - Calibration curve on the UV-Vis Spectrophotometer

### 3.5 Flue gas analysis

The sampling point to extract the flue gas is located midway on the combustion chamber. The flue gas from the combustion chamber follows the sample path to a set of three impingers containing distilled water immersed in an ice cold bath. The water in the exhaust gas sample is condensed in these impingers and the gas out of the impingers is a dry gas, which is then analyzed by the micro GC. The NO<sub>x</sub> values were measured using a NO<sub>x</sub> analyzer by Thermo Scientific, Model 42i series based on the chemiluminescence technology, which was calibrated before each test. The analyzer used for the measurements is shown in Fig 3.14. The NO<sub>x</sub> data was collected for each of the condition

run at the burner. The burner is allowed to attain steady state before starting to record the data. Data is recorded for 10 minutes at each condition with a sampling rate of 10 seconds. Average of all this data is then assumed as the representation of NO<sub>x</sub> at that condition with error bars in the plots indicating the minimum and maximum variation.



**Fig 3.14 - Thermo scientific NO<sub>x</sub> analyzer**

## CHAPTER 4: RESULTS AND DISCUSSIONS

### 4.1 Test matrix

Tests were conducted for five different feedstock and the compositions of both producer gas and flue gas were measured. Different biomass will result in different producer gas compositions. For the same feedstock, the burner was operated at various fuel flow rates. For each flow rate (i.e., heat rate), various equivalence ratios were tested by adjusting the air flow rate. The test matrix for different feedstocks are shown in Table 4.1. All the combustion test conditions were in the lean mixture range with the richest mixture being close to stoichiometry. The combustion chamber can reach very high temperature when using stoichiometric mixtures, reaching the upper limits of temperature for the present combustion chamber material. Hence richer mixtures were avoided. The producer gas flow rates were chosen in the bandwidth of the gas flow meter to ensure accurate measurement. The feedstocks tested have different nitrogen contents. All the tests were performed with the gasifier operating at 815 °C. Notice that the specific burner test conditions (e.g., equivalence ratios, heat rates) are not exactly the same for different feedstock, as will be seen in Fig. 2. The specific operating conditions of the burner were determined considering the limitations of the system and operating points of interest. In general, at high heat rates, more test points were based on the lean operating conditions to prevent from overheating the combustion chamber.

**Table 4.1 - Test Conditions**

Feedstock	Nitrogen content (%)	Producer gas flow rate, pounds per hour (pph)	Burner Eq. Ratio
Wood	0.14	50 – 250	1.2 – 3.0
Wood+7%DDGS	0.37	50 – 250	1.0 – 2.1
Wood+13%DDGS	0.66	50 – 250	1.0 – 2.2
Wood+20%DDGS	0.95	50 – 250	1.0 – 2.2
Wood+40%DDGS	1.75	50 – 250	1.0 – 2.3
Wood+70%DDGS	2.81	50 – 250	1.0 – 2.2
Yellow Corn	1.05	50 – 250	1.0 – 2.2

**Table 4.2 - Proximate and ultimate analysis of different biomass feedstock**

Feedstock	Wood	Wood+7% DDGS	Wood+13% DDGS	Wood+20% DDGS	Wood+40% DDGS	Wood+70% DDGS	Yellow Corn
	<b>Proximate analysis (wt %)</b>						
Fixed Carbon	16.81	17.14	17.27	17.48	17.40	15.58	15.12
Volatiles	75.11	75.76	75.18	74.14	71.93	71.20	70.47
Moisture	6.25	6.22	6.02	6.24	8.20	10.17	13.37
Ash	1.83	0.88	1.53	2.13	2.47	3.04	1.04
	<b>Ultimate Analysis (wt %)</b>						
C	46.56	46.48	46.01	45.50	45.15	44.62	39.71
O	46.13	46.08	45.68	44.98	44.05	42.85	51.35
H	6.24	6.40	6.43	6.40	6.72	7.05	7.01
N	0.14	0.37	0.66	0.95	1.75	2.81	1.05
S	0.02	0.06	0.10	0.13	0.23	0.42	0.08

The proximate and ultimate analysis for each feedstock is shown in Table 4.2. These analyses are very important to determine the fuel nitrogen present in the feedstock. This helps in understanding the conversion of this nitrogen into ammonia and finally to NO<sub>x</sub> in the burner.

## 4.2 Producer gas compositions

The feedstock are gasified under fuel rich conditions to generate producer gas, which mostly comprises of nitrogen (N<sub>2</sub>), carbon monoxide (CO), hydrogen (H<sub>2</sub>), methane (CH<sub>4</sub>), carbon dioxide (CO<sub>2</sub>), water (H<sub>2</sub>O), ammonia (NH<sub>3</sub>), and other hydrocarbons. The wet gas composition of the producer gas using various biomass feedstock is shown in Table 4.3. Note that the producer gas composition (except ammonia) was measured using a micro GC, which indicated steady reading throughout the measurement. For ammonia, due to the complexity in the measurement, one sample was taken and analyzed for each feedstock. As a result, only a set of gas composition data corresponding to each feedstock are reported in Table 4.3. It can be seen that ammonia concentration increases with increased nitrogen content in the feedstock. The gasifier was maintained at a steady state of 815 °C for all the different operating conditions of the burner.

**Table 4.3 - Producer gas composition using different biomass feedstock**

Feedstock	% wet volumetric basis						
	Wood	Wood+7% DDGS	Wood+13% DDGS	Wood+20% DDGS	Wood+40% DDGS	Wood+70% DDGS	Yellow corn
<b>Components of Producer gas</b>							
Nitrogen (N <sub>2</sub> )	39.02	39.67	40.16	39.86	41.51	50.57	38.97
Carbon monoxide (CO)	16.91	17.74	16.26	15.86	12.55	12.54	13.63
Hydrogen (H <sub>2</sub> )	11.33	9.54	10.46	8.97	7.01	4.39	4.63
Carbon dioxide (CO <sub>2</sub> )	13.56	14.57	14.88	14.01	12.87	10.98	11.40
Methane (CH <sub>4</sub> )	5.27	6.32	5.88	5.68	5.17	4.50	3.93
Ethane (C <sub>2</sub> H <sub>6</sub> )	0.26	0.32	0.30	0.25	0.29	0.43	0.20
Ethylene (C <sub>2</sub> H <sub>4</sub> )	1.18	1.82	1.66	1.83	1.93	2.36	1.83
Acetylene (C <sub>2</sub> H <sub>2</sub> )	0.07	0.11	0.10	0.12	0.10	0.15	0.18
Propane (C <sub>3</sub> H <sub>8</sub> )	0.07	0.13	0.11	0.10	0.17	0.18	0.13
Ammonia (NH <sub>3</sub> )	0.06	0.13	0.18	0.23	0.24	1.15	0.54
Water (H <sub>2</sub> O)	9.97	10.67	10.64	13.58	18.63	12.33	24.14
Lower heating value (MJ/kg)	5.58	5.95	5.69	5.52	4.96	4.83	4.49
Adiabatic flame temperature (K)	1932	1959	1932	1908	1822	1825	1761

### 4.3 Emissions using natural gas

Baseline tests were performed for the burner using natural gas as the fuel and the results are shown in Fig. 2a. The reported NO<sub>x</sub> emissions data have been normalized based on 3% oxygen level in the exhaust using the following equation.

$$NOx @ 3\% O_2 = NOx \text{ Raw data} \times \frac{(1-0.03)}{(1-\%O_2)} \quad (1)$$

The above adjustment in reporting flue gas NO<sub>x</sub> emissions is to consider the dilution effect and is a common practice in the burner industry. For instance, at very lean conditions (i.e., high oxygen concentrations in the exhaust), the measured raw NO<sub>x</sub> emissions have been diluted by the excess air. By using Eq. (1), the reported NO<sub>x</sub> @ 3% O<sub>2</sub> will be higher than the raw data, thus resulting in a fair comparison. The NO<sub>x</sub> values are also plotted in g/kW-hr. This is a standard way to compare different combustion systems, especially in the engine industry, having different rated power. This NO<sub>x</sub> reported is independent of the fuel flow rate as indicated below in equation 2.

$$NOx \left( \frac{g}{kW-hr} \right) = \frac{y_{NOx}}{HV} \times \left( \frac{A}{F} + 1 \right) \quad (2)$$

where  $y_{NOx}$  is the mass fraction of NO<sub>x</sub> in the flue gas

HV is the heating value of the producer gas

$\frac{A}{F}$  is the air-fuel ratio

For the same heat rate, the NO<sub>x</sub> emissions variation with equivalence ratio is small. Here the equivalence ratio is defined as the ratio of the actual air-fuel ratio to the stoichiometric air-fuel ratio. That is, an equivalence ratio greater than 1.0 indicates a lean mixture. It is known that the thermal NO<sub>x</sub> is mainly a function of the adiabatic flame temperature. In a premixed flame, the stoichiometric mixture produces the highest flame temperature which in general will result in the highest thermal NO<sub>x</sub> emissions. However, it should be noticed

that the present burner is based on non-premixed combustion in which fuel and air are introduced into the burner at different stages. It is believed that a diffusion flame is established in the burner because the fuel and air are not premixed. In a diffusion flame, the exhaust NO<sub>x</sub> emissions are less sensitive to the overall equivalence ratio. Thus, NO<sub>x</sub> emissions do not vary significantly with the equivalence ratio, as shown in Fig. 4.1. The graphs are present in terms of NO<sub>x</sub> at 3% exhaust oxygen and also in terms of g/kW-hr which is independent of the fuel flow rate. The adiabatic flame temperature for natural gas is 2325 K calculated from the EES (Engineering equation solver) code. Nonetheless, relatively speaking, NO<sub>x</sub> emissions seem to reach a maximum at slightly lean conditions due to the availability of excess oxygen to produce NO<sub>x</sub>. On the other hand, NO<sub>x</sub> emissions increase noticeably as the heat rate is increased. This outcome is attributed to the increased thermal loading inside the combustion chamber due to the higher fuel flow rates, as supported by the results of NO<sub>x</sub> in g/kW-hr (which is independent of fuel flow rate). At higher thermal loading, the chamber will reach a higher temperature, which in turn causes the overall gas temperature to rise, hence contributing to the increased NO<sub>x</sub> emissions.

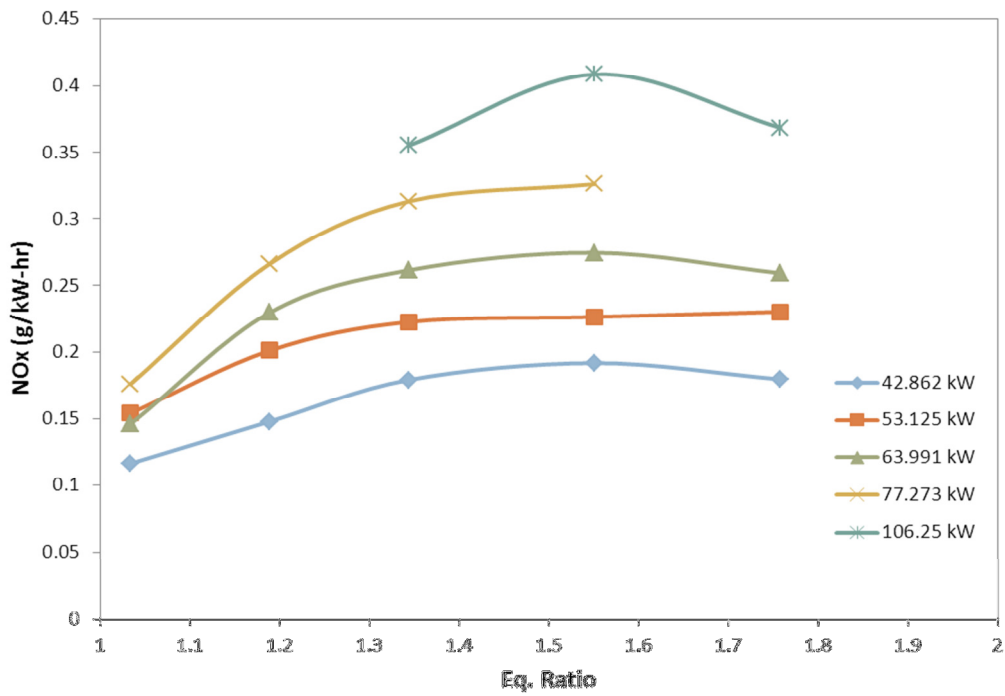
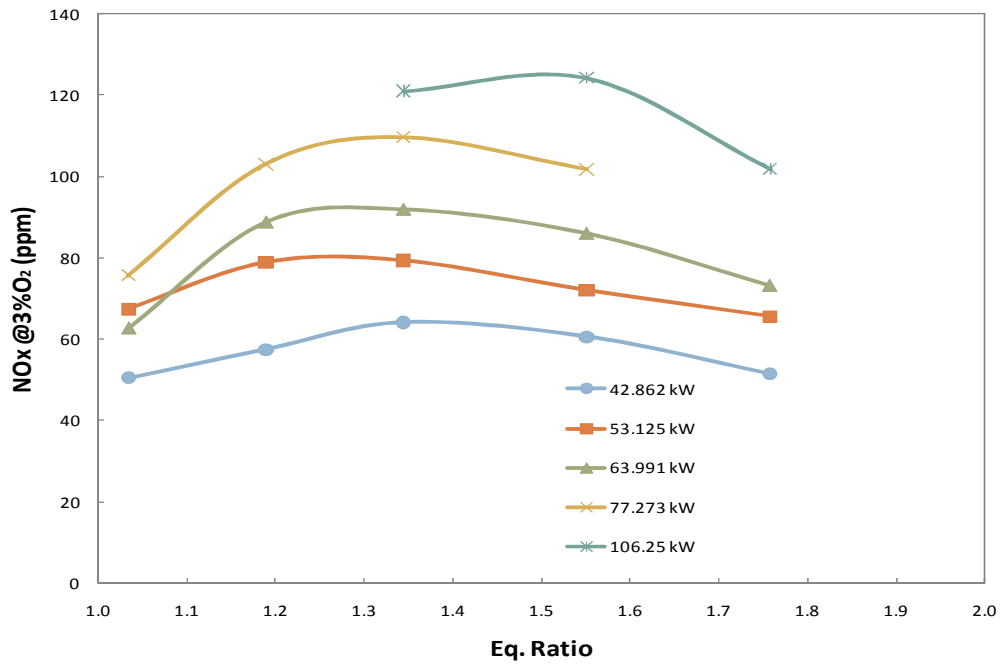


Fig. 4.1 - NO<sub>x</sub> variation with equivalence ratio for different heat rates using natural gas

#### 4.4 Emissions using wood

Fig. 4.2 shows the NO<sub>x</sub> emissions using producer gas resulting from wood gasification. The NO<sub>x</sub> emissions increase with increased fuel flow rates for a given equivalence ratio. Table 4.1 shows that the nitrogen content in the present wood feedstock is 0.13% and ammonia is approximately 600 ppm in the producer gas. This amount of ammonia is significant enough to increase the NO<sub>x</sub> emissions in the combustion exhaust. As compared to Fig. 2a using natural gas, the exhaust NO<sub>x</sub> emissions using wood-derived producer gas are noticeably higher. It should be noted that producer gas has lower energy content and lower flame temperature than natural gas. Thus, the increase in NO<sub>x</sub> emissions is due to “fuel NO<sub>x</sub>” resulting from combustion of fuel-bound nitrogen, i.e., ammonia in this case. On the other hand, similar to natural gas, NO<sub>x</sub> emissions increase as the heat rate increases due to the higher combustion chamber temperature as more fuel is burned. Additionally, the increased amount of ammonia in the fuel flow can also increase fuel NO<sub>x</sub> emissions.

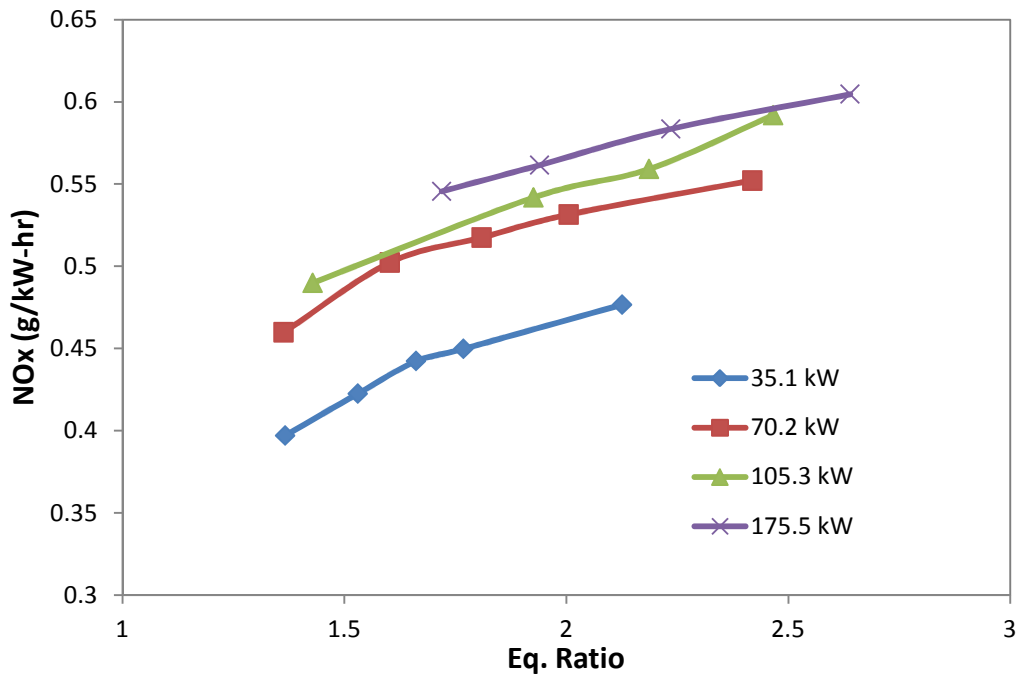
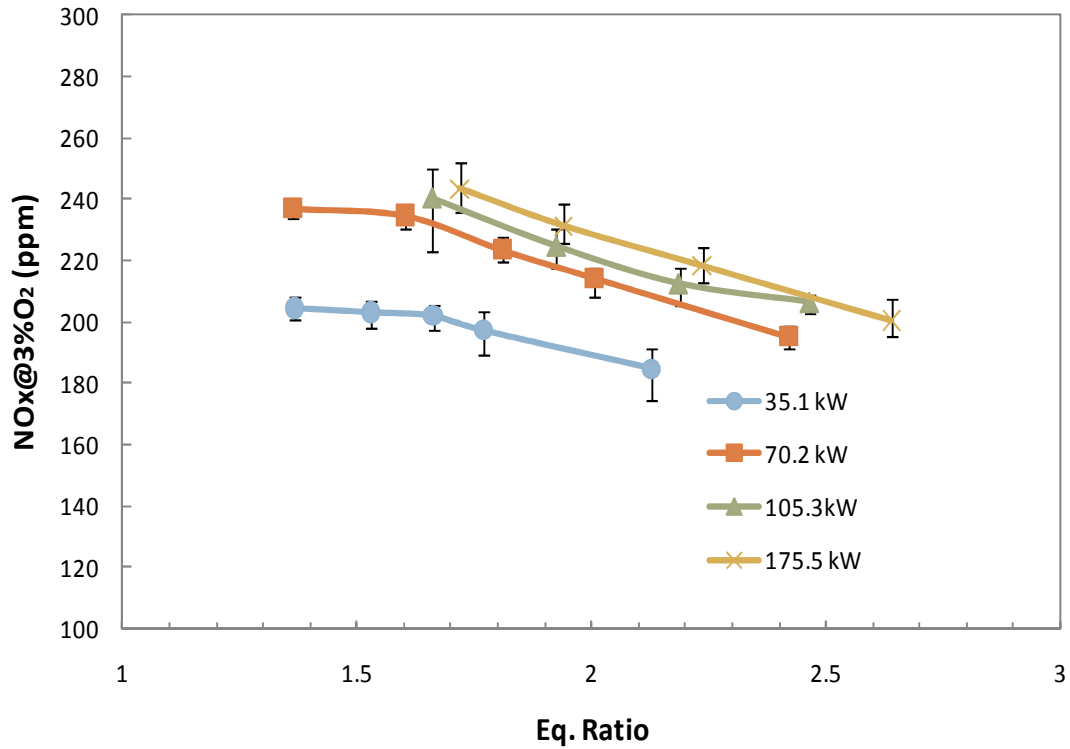


Fig 4.2 - NOx emissions using producer gas resulting from gasifying wood

#### 4.5 Emissions using wood with 7% DDGS

As the biomass feedstock contains more nitrogen, it is expected that producer gas will contain more ammonia which, in turn, results in higher NO<sub>x</sub> emissions. Fig 4.3 shows the NO<sub>x</sub> emissions corresponding to wood with 7% DDGS. As can be seen, the magnitude of NO<sub>x</sub> is about 100 to 200 ppm higher than that using wood. This increase in NO<sub>x</sub> emissions is attributed to the higher nitrogen content in the biomass feedstock, thus resulting in higher ammonia in the producer gas. It can also be seen that the difference in NO<sub>x</sub> emissions for different heat rates is more significant than the cases using wood or natural gas. The reason is due to the increased amount of ammonia in producer gas that leads to the significant increase in fuel NO<sub>x</sub> emissions after combustion. Effects of fuel flow rate on the NO<sub>x</sub> emissions become more significant for feedstock with high nitrogen content.

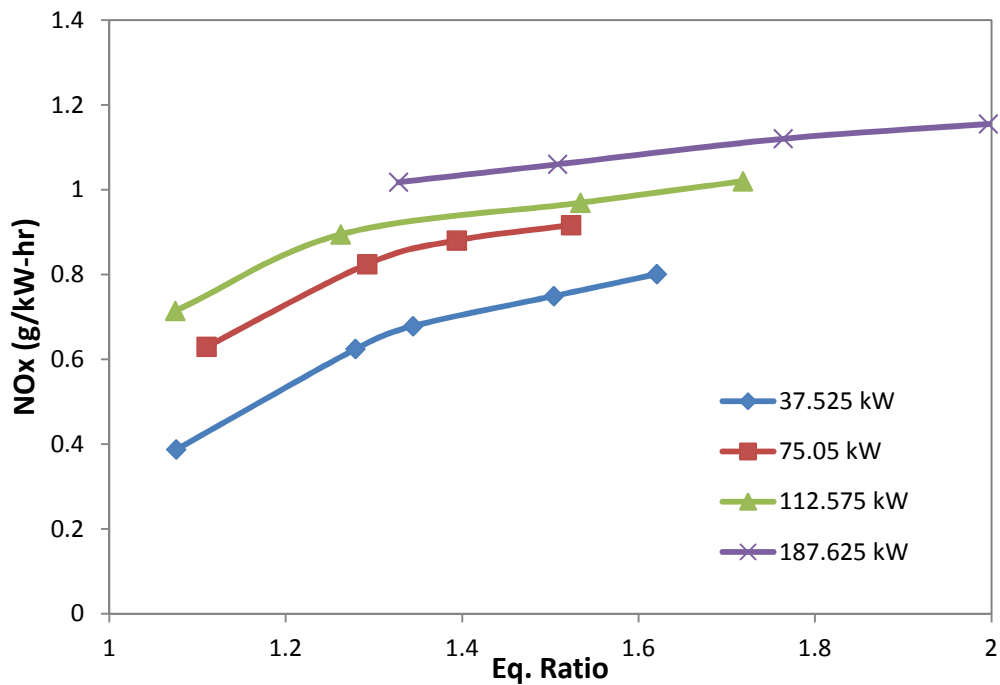
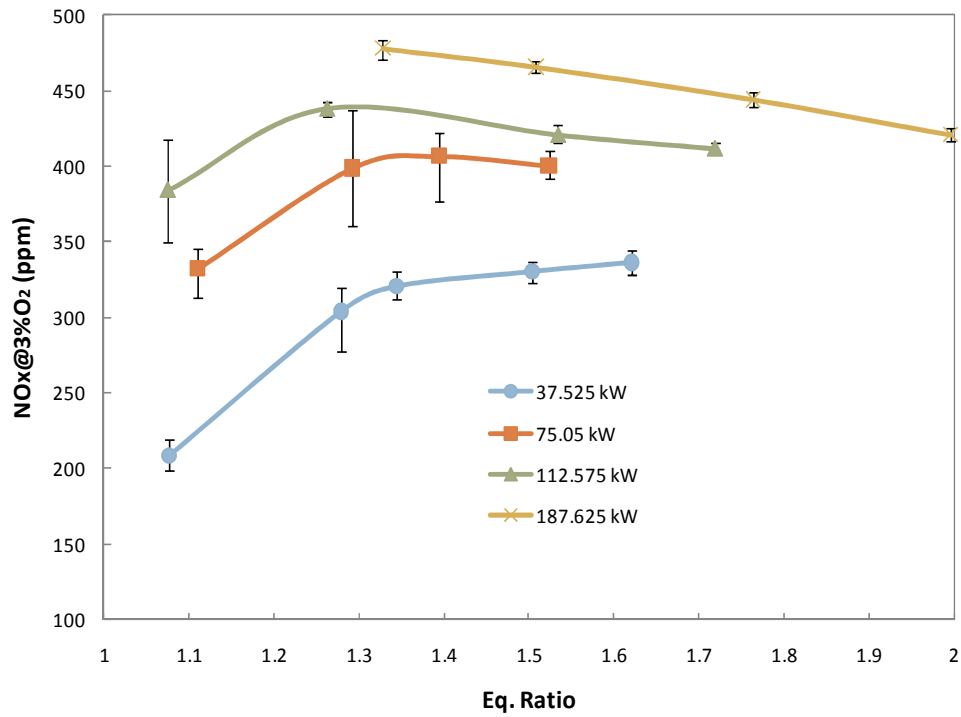
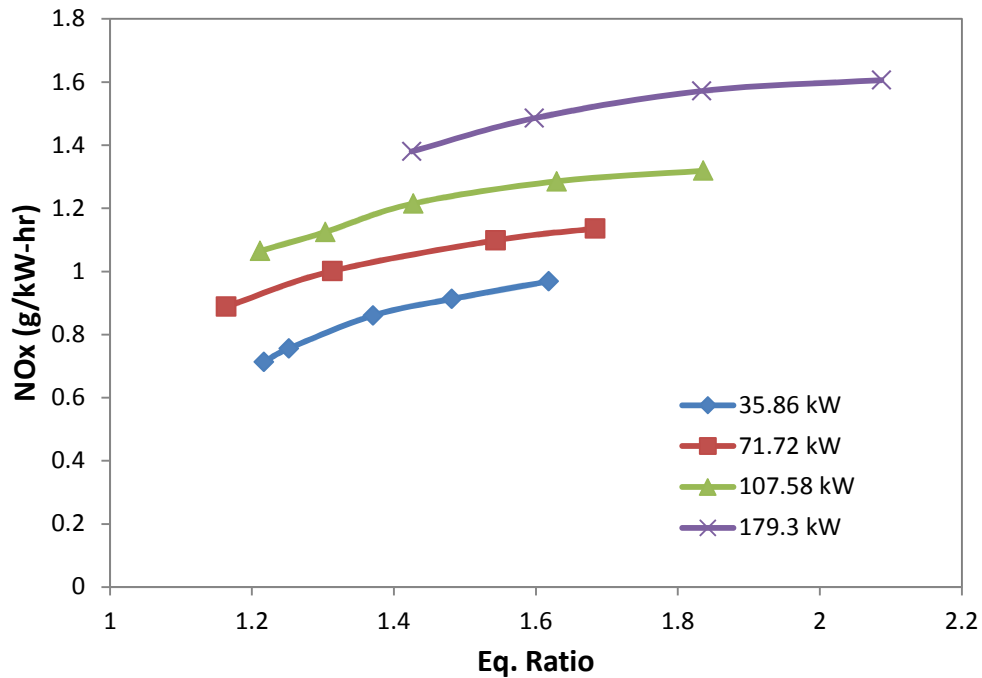
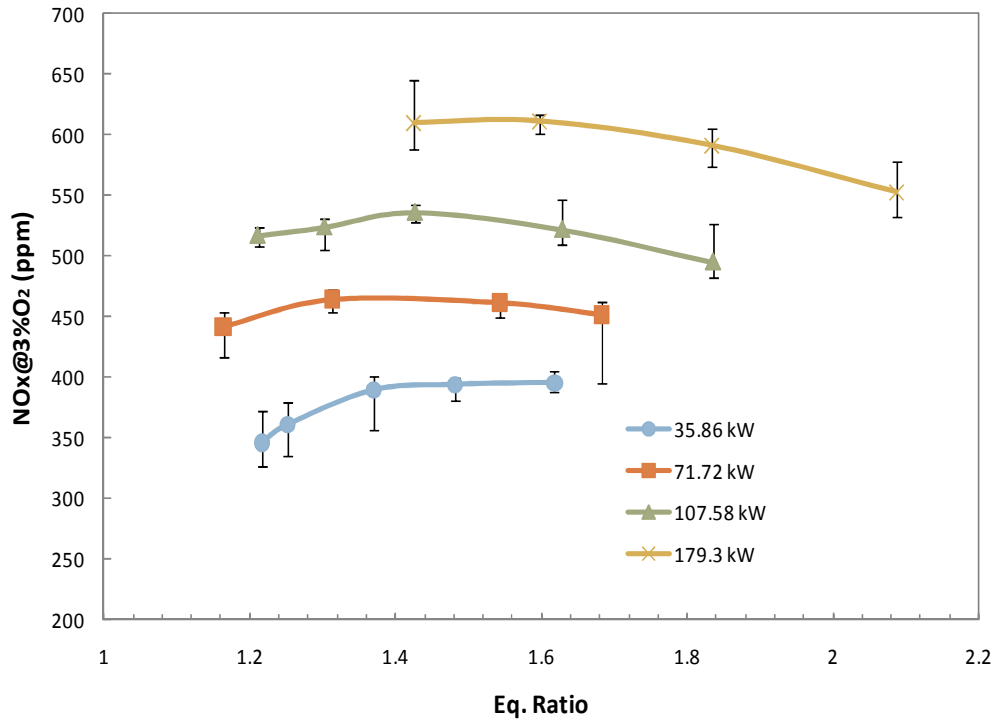


Fig 4.3 - NOx emissions using producer gas resulting from gasifying wood with 7%

DDGS

#### 4.6 Emissions using wood with 13% DDGS

Table 4.3 shows that the ammonia in producer gas increases with the nitrogen content in the biomass feedstock. NO<sub>x</sub> emissions using wood with 13% DDGS as seen in Fig 4.4 are higher compared to the previous cases. The higher nitrogen content leads to more fuel NO<sub>x</sub> formation and hence the overall NO<sub>x</sub> increases. In these cases, it is believed that the fuel NO<sub>x</sub> is the main contributor to the total NO<sub>x</sub> emissions since the heating value and flame temperature of producer gas are lower than those using natural gas and yet NO<sub>x</sub> emissions are much higher.



**Fig 4.4 - NOx emissions using producer gas resulting from gasifying mixtures of wood and 13% DDGS**

#### 4.7 Emissions using wood with 20% DDGS

The nitrogen content of wood with 20% DDGS is very close to that of seed corn (i.e., approximately 1.05%), shown in Table 4.2. The NO<sub>x</sub> emissions using wood with 20%DDGS, as shown in Fig 4.5, have higher NO<sub>x</sub> values compared to wood with 13%DDGS as expected. It is evident that the NO<sub>x</sub> emissions continue to increase as the nitrogen content in biomass feedstock increases. The NO<sub>x</sub> represented in g/kW-hr, being independent of fuel flow rate, still seems to be varying with the fuel flow rate. This trend is seen for all the cases of producer gas. This is due to the NO<sub>x</sub> values varying with the fuel flow rate and hence is attributed to the presence of ammonia in the producer gas.

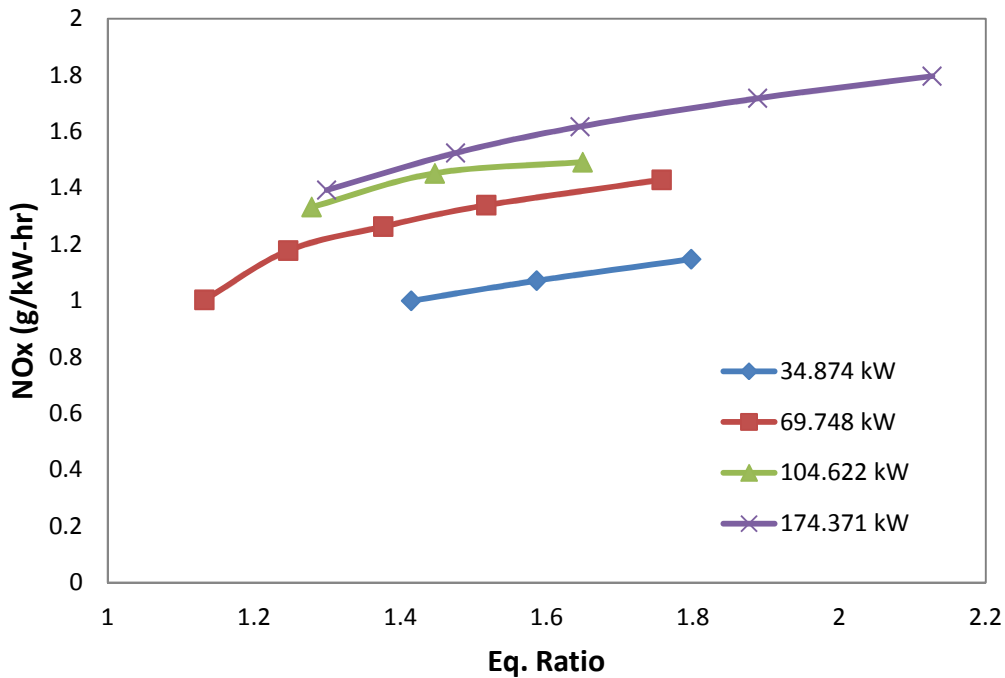
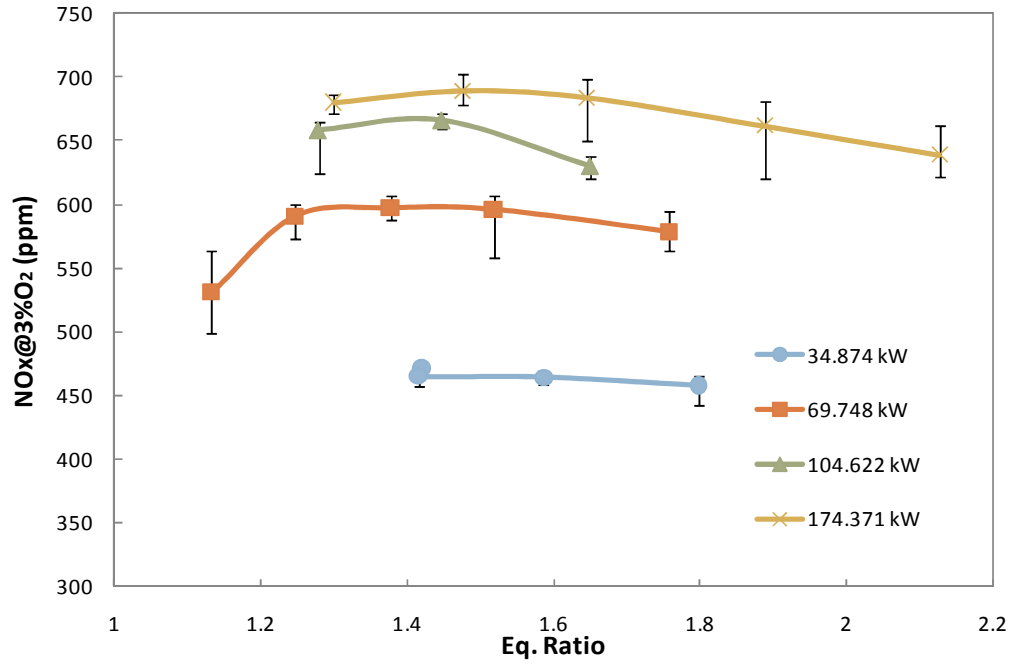


Fig 4.5 - NOx emissions using producer gas resulting from gasifying mixtures of wood and

20% DDGS

#### **4.8 Emissions using wood with 40% DDGS**

The mixture of wood and 40%DDGS has relatively high nitrogen content and subsequently results in high NO<sub>x</sub> emissions when producer gas is burned as shown in Fig 4.6. Such high NO<sub>x</sub> emissions may make it impractical to utilize such feedstock for heat and power generation under the emission regulations even for burners with good combustion design.

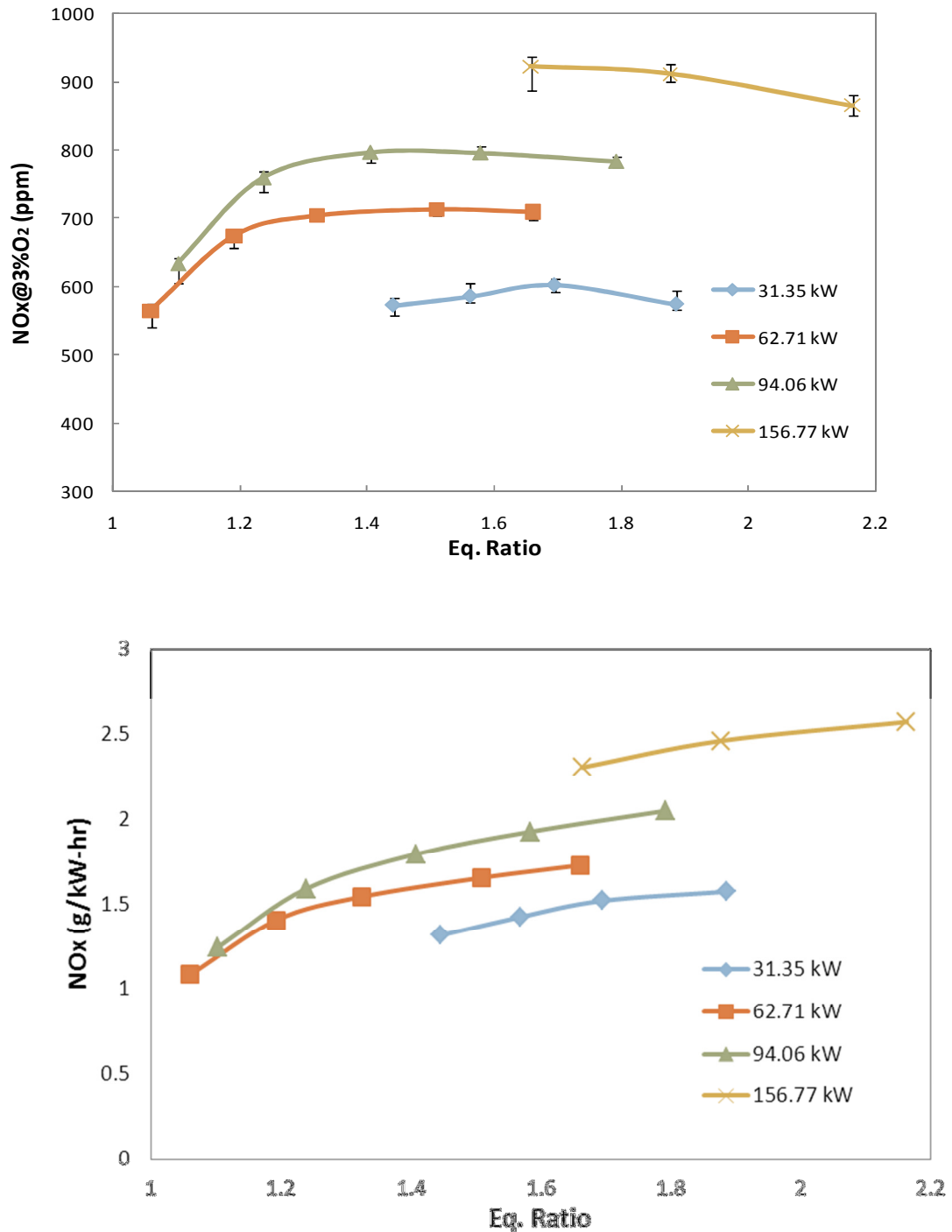


Fig. 4.6 - NO<sub>x</sub> emissions using producer gas resulting from gasifying mixtures of wood and 40% DDGS

#### 4.9 Emissions using wood with 70% DDGS

As seen in Table 4.2, the nitrogen content in this feedstock is about 2.5%, and hence it is expected that there will be higher concentrations of ammonia in the producer gas as shown in Table 3. This feedstock could not be pelletized effectively and was too moist which prevented it from remaining as a pellet. This resulted in uneven feed of the biomass to the gasifier resulting in varying composition of producer gas. Thus the conditions at the burner were not steady and the data collected can be considered reasonable only for the producer gas as it was sampled for a longer duration and represents an average composition of producer gas. The plots of NO<sub>x</sub> shown in Fig 4.7 present the range of NO<sub>x</sub> for wood with 70%DDGS and such high values make it impossible to consider using it as a feedstock.

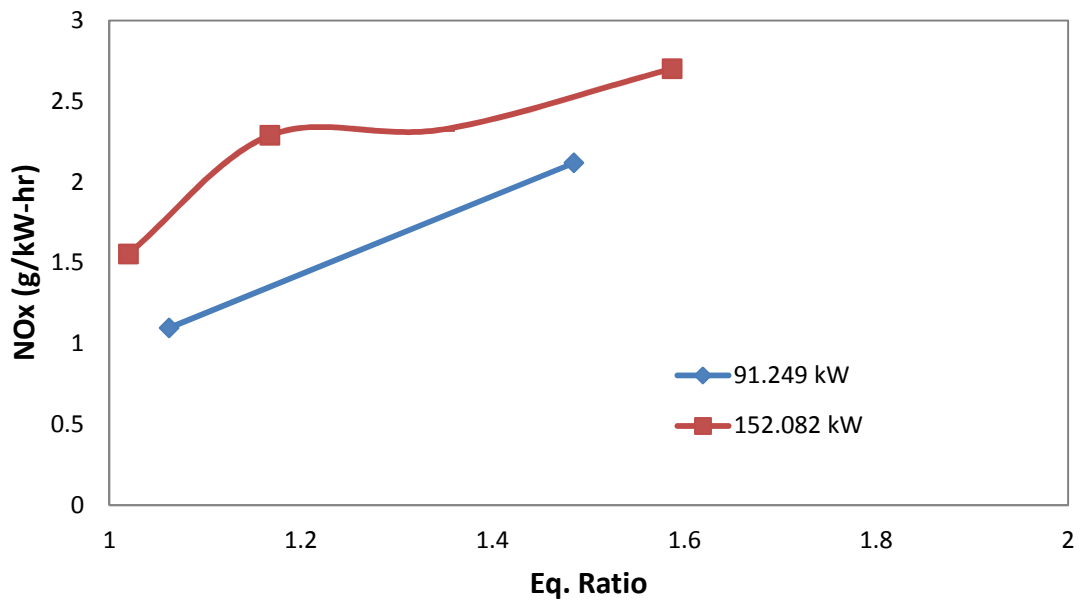
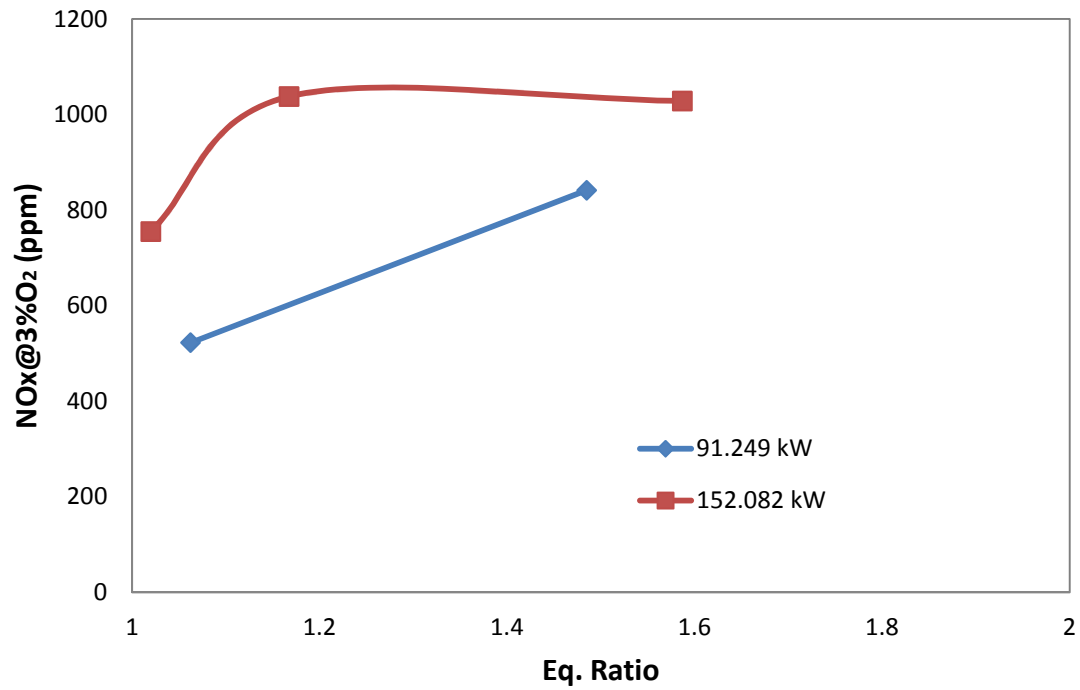


Fig 4.7 - NOx emissions using producer gas resulting from gasifying mixtures of wood and 70% DDGS

#### 4.9 Emissions using yellow corn

Yellow corn is a standard biomass feedstock used for most of the applications. Yellow corn was gasified along with the other feedstocks so that it could provide a basis to compare our analysis results with the literature. Yellow corn has nitrogen content comparable to that of wood with 20% DDGS as shown in Table 4.2. This results in a considerable amount of ammonia in the producer gas forming a precursor to fuel NO<sub>x</sub>. The trends for NO<sub>x</sub> emissions at different equivalence ratios and for different heat rates are shown in Fig 4.8.

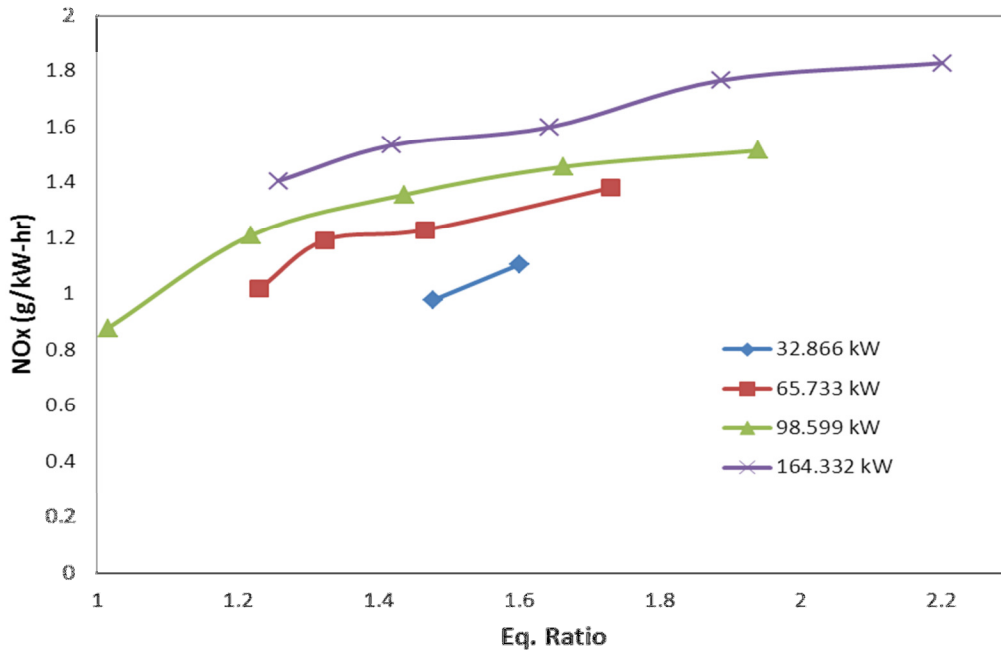
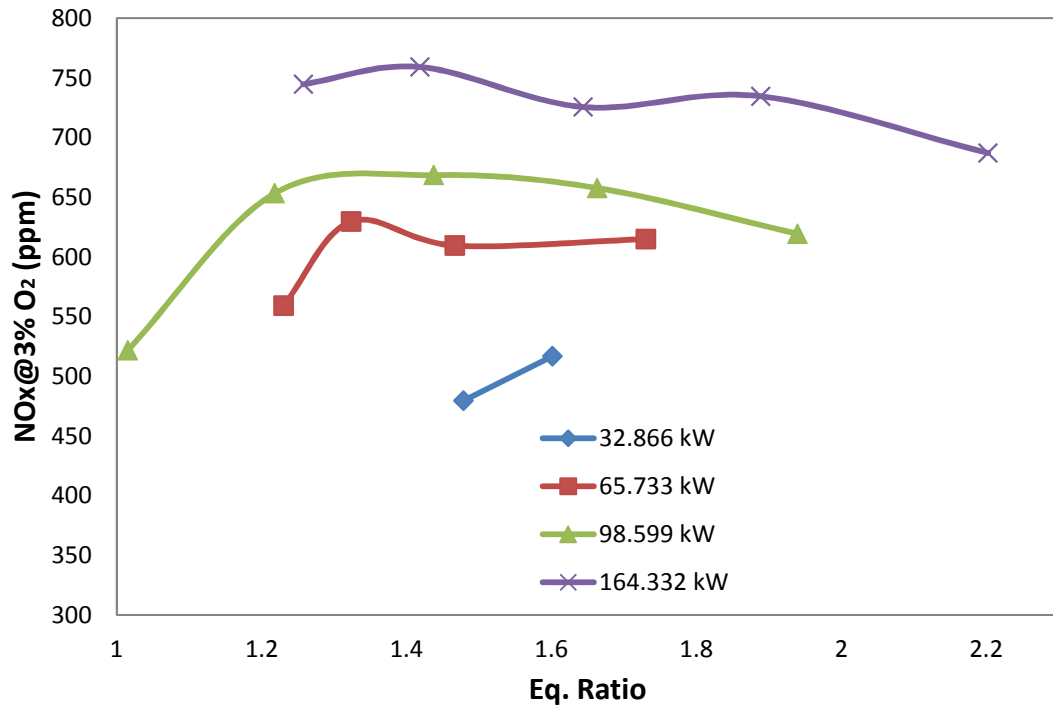
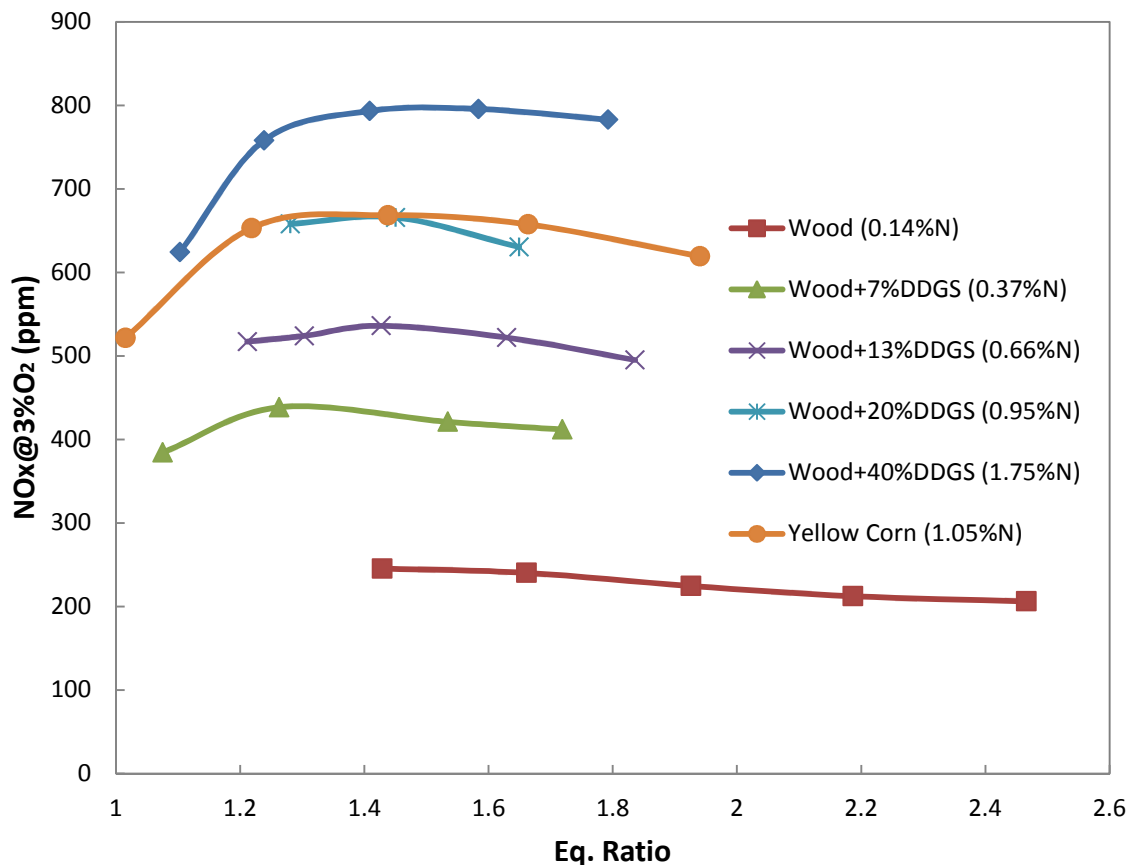


Fig 4.8 - NOx emissions using producer gas resulting from gasifying yellow corn

#### 4.11 Discussions

There were a few problems encountered during the testing phases with one of them being the condensation of tars on the spark plug. The producer gas enters the burner at a temperature slightly below 350 °C. The tars begin condensing at temperatures ranging between 80 °C and 200 °C. These tars collect on the spark plugs and will eventually clog them. Hence spark plugs had to be replaced once in every three to four days of run. During the present measurements, it was found that it is of great challenge to measure ammonia concentration in the hot producer gas stream (with a temperature approximately 325 °C at the measurement point after gas clean-up). Initially a mass spectrometer (MS) was used, but the various contaminants in producer gas have caused numerous equipment malfunctions. The sampling tube of the mass spectrometer has a diameter of 1/16 inch, which makes it difficult to sample producer gas containing particulates like chars. Particulate filters with meshes of micron size were employed to overcome this issue. The major hurdle encountered was that ammonia and water have very similar molecular weights, causing extreme difficulties in distinguishing between these two species in the MS. It was also found impossible to calibrate the MS for water due to the high moisture content in producer gas (shown in Table 4.3). As a result, it was agreed to first filter out the tars with sanoprene tubes and then condense the water in the impingers. The rationale behind this was to use the sample collected in the sanoprene tube for tar analysis and the sample collected in the impingers for water and ammonia analysis. But it was found that some of the salts were lost in the sanoprene tubes along with the tars. Hence these salts

were being un-accounted for in the calculation of ammonia. As a result, the IEA sampling method was employed for ammonia measurement in the hostile environment encountered in the present application. This ensured that the salts are captured effectively and the three impingers downstream make sure that there is no ammonia slip.



**Fig 4.9 - Effect of fuel nitrogen on NO<sub>x</sub> emissions for producer gas flow rate of 150 pph**

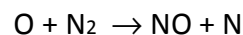
It was found that the concentration of ammonia is the highest in the last three impingers placed downstream of the IEA sampling method. This could be attributed to the fact that the IEA impingers contain IPA in them, which does not dissolve salts easily. Hence limited amount of ammonia is captured in the six IEA method impingers. The presence of

water and 0.05% HCl in the three impingers downstream readily dissolves all the salts. The high vapor pressure of ammonia in these impingers may lead to loss of ammonia during the collection and roto-evaporation process, if not handled correctly. The containers also need to be stored in a cold environment to reduce the loss of ammonia in the form of vapor. The loss can be avoided by storing the samples at  $0 - 5^{\circ}\text{C}$  and measuring for ammonia as soon as possible to avoid potential storage losses. The present results show that ammonia concentrations tend to follow an increasing trend with the increase in the nitrogen content in the feedstock. Though some of the feedstocks report low ammonia concentration, it is understood that these feedstocks were run at the early stage of the test and not much detail was known regarding their storage and handling. The experiments for later feedstocks show good agreement with literature for the similar nitrogen content in the feedstock. Thus, the relationship between the nitrogen content in biomass feedstock, ammonia concentration in producer gas, and NO<sub>x</sub> emissions from the burner is discussed as follows.

Fig. 4.9 shows the variation of NO<sub>x</sub> emissions with different equivalence ratios for all the different biomass feedstocks at a fuel flow rate of 150 pph (pounds per hour), corresponding to a heat rate of approximately 100 kW. There is a tendency for the peak NO<sub>x</sub> values for some of the feedstock to shift towards leaner mixtures as the percentage of nitrogen in the feedstock is increased. This can be explained as follows. As the percentage of nitrogen is increased in the feedstock, the corresponding ammonia concentration in producer gas increases. Since the fuel NO<sub>x</sub> results from the oxidation of ammonia in producer gas, the higher the ammonia concentration is, the more oxygen is required to

react with ammonia to form NO<sub>x</sub>. Thus, the excessive oxygen at lean conditions will further result in high NO<sub>x</sub> emissions. From Fig. 4.9, it can be seen that wood with 40%DDGS has the maximum NO<sub>x</sub> at an equivalence ratio of 1.5 as compared to wood with 7%DDGS which has the peak NO<sub>x</sub> at an equivalence ratio of 1.25. This tendency of shifting the peak NO<sub>x</sub> value is apparent for wood with 7%DDGS, wood with 20%DDGS, wood with 40%DDGS and yellow corn. Future tests can be conducted over a wider range of equivalence ratio to help identify the trend. Also, it has to be noted that yellow corn and wood+20%DDGS have similar percentage of nitrogen in the raw biomass feedstock and have very close NO<sub>x</sub> values under similar conditions of run.

It is also worth investigating the contributions of thermal NO<sub>x</sub> and fuel NO<sub>x</sub> in producer gas combustion. In the present setup, NO<sub>x</sub> emissions using natural gas ranges between 50 to 130 ppm, which are entirely due to thermal NO<sub>x</sub>, shown in Fig. 4.1. The combustion temperature attained using producer gas is lower than that using natural gas due to its low energy content, the adiabatic temperatures for each feedstock is shown in Table 3. Therefore, thermal NO<sub>x</sub> formed using producer gas will be lower than that using natural gas and usually negligible as thermal NO<sub>x</sub> is significant only above 1800K. Also, it is understood that the thermal NO<sub>x</sub> is formed mainly by the following reaction (Glarborg et al., 2003).



In the presence of ammonia in the fuel, the NO formed from the oxidation of fuel nitrogen tends to react with the nitrogen free radical and reverse the above reaction. The

thermal NO<sub>x</sub> for fuels with nitrogen species is only dominant beyond 2200K because of this effect (Pershing, 1976). In addition, the heat loss to the surroundings would lower the actual flame temperature and hence limit the formation of thermal NO<sub>x</sub>. However, by comparing Fig 4.1 and Fig 4.2, NO<sub>x</sub> emissions increase from 50 – 130 ppm using natural gas to 190 – 250 ppm using wood-derived producer gas. Hence, the majority of NO<sub>x</sub> formed during the combustion of producer gas is believed to be predominantly fuel NO<sub>x</sub>. For the feedstocks tested in this study, it was found that the effect of nitrogen compounds (i.e., ammonia) in the producer gas on NO<sub>x</sub> emissions is very significant, particularly for feedstock with high concentrations of DDGS. Additionally, as can be seen in Fig 4.9, for the same equivalence ratio, NO<sub>x</sub> emissions increase significantly as the nitrogen content in the feedstock increases. As discussed above, since the thermal NO<sub>x</sub> for producer gas combustion can be relatively insignificant, the increase in NO<sub>x</sub> emissions is likely due to fuel NO<sub>x</sub>, resulting from ammonia combustion. It is noted that the change of NO<sub>x</sub> with nitrogen content in the biomass feedstock is not a constant and the rate of increase in NO<sub>x</sub> seems to be reducing with increasing nitrogen content as shown in Fig 4.10. This is explained by the fact that at higher ammonia concentrations in the fuel, NO<sub>x</sub> is reduced to nitrogen and hence higher the ammonia, more dominant is the de-NO<sub>x</sub> mechanism (Koger, 2005). This is the same principle used in the selective catalytic reduction (SCR) for the aftertreatment systems.

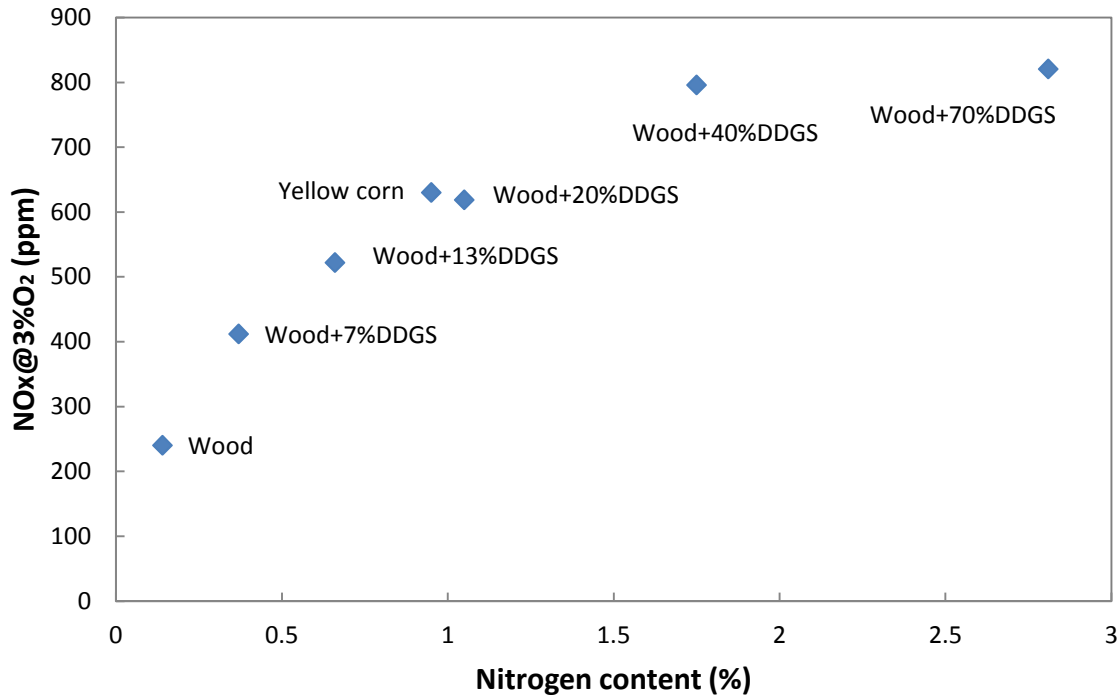


**Fig 4.10 - Change in NO<sub>x</sub> for different nitrogen contents in the biomass feedstock**

It is known that the thermal NO<sub>x</sub> is mainly a function of flame temperature. The increase in NO<sub>x</sub> emissions at the higher natural gas flow rate (Fig. 4.1) is believed to be due to the characteristic of the diffusion flame. As the fuel flow rate is increased, for the same equivalence ratio, the flame length increases. The increase in flame length increases the area of interaction between fuel and air, hence increasing the NO<sub>x</sub> emissions. The Zeldovich mechanism for thermal NO<sub>x</sub> states that the thermal NO<sub>x</sub> formation increases linearly with residence time. As the flow rate of natural gas is increased, the residence time and hence the NO<sub>x</sub> formation decreases. The variation in fuel flow rates for natural gas as

seen in Fig 4.1 is not significant enough to let the residence time have any major effect on the NO<sub>x</sub> formation. Thus there is an overall increase in the NO<sub>x</sub> emissions with increasing fuel flow rate. It can be observed from Fig 4.2 to Fig 4.8 that for a given equivalence ratio, NO<sub>x</sub> emissions for producer gas increases significantly with increasing fuel flow rate. As discussed earlier, the increase in fuel flow rates, increases the flame length and hence the area of reaction between fuel (ammonia) and air. In the conditions tested for producer gas, the variation in the fuel flow rates is significant and hence the effect of residence time on the NO<sub>x</sub> formation cannot be neglected. At high residence times (i.e. low fuel flow rates), there is sufficient time for ammonia (from the fuel) to react with NO<sub>x</sub> formed (de-NO<sub>x</sub> mechanism) and hence converting it to nitrogen. Hence we see low NO<sub>x</sub> emissions at lower flow rates. Thus in the case of fuel NO<sub>x</sub>, the residence time seems to be inversely proportional to the NO<sub>x</sub> formation. The difference in the adjacent NO<sub>x</sub> curves for different heat rates in Fig 4.2 to Fig 4.8 is larger than that in Fig 4.1, further illustrating the importance of fuel NO<sub>x</sub> in the biomass-derived producer gas combustion.

Figure 4.11 shows the relationship between the nitrogen content in biomass, ammonia concentration in producer gas, and NO<sub>x</sub> emissions in the flue gas. The data is based on a fuel flow rate of 150 pph and an equivalence ratio of 1.65. Since there is a lot more confidence in the results of ammonia concentrations for wood, wood+70%DDGS and yellow corn, these feedstocks have been selected to show the nitrogen conversion path. As the nitrogen content in the biomass feedstock increases, the corresponding ammonia concentrations and NO<sub>x</sub> emissions increase as expected. The plot in Fig 4.12 confirms the reduction in the slope of NO<sub>x</sub> with increasing ammonia. This is because at higher ammonia

concentrations, the de-NO<sub>x</sub> effect becomes significant and hence lowering the conversion of ammonia to NO<sub>x</sub>. It is anticipated that there will be practical constraints on the nitrogen content in biomass in order to limit the NO<sub>x</sub> emissions level when the producer gas is used for combustion. These constraints will depend on the design of the combustion device and the exhaust after-treatment system for NO<sub>x</sub> reduction.

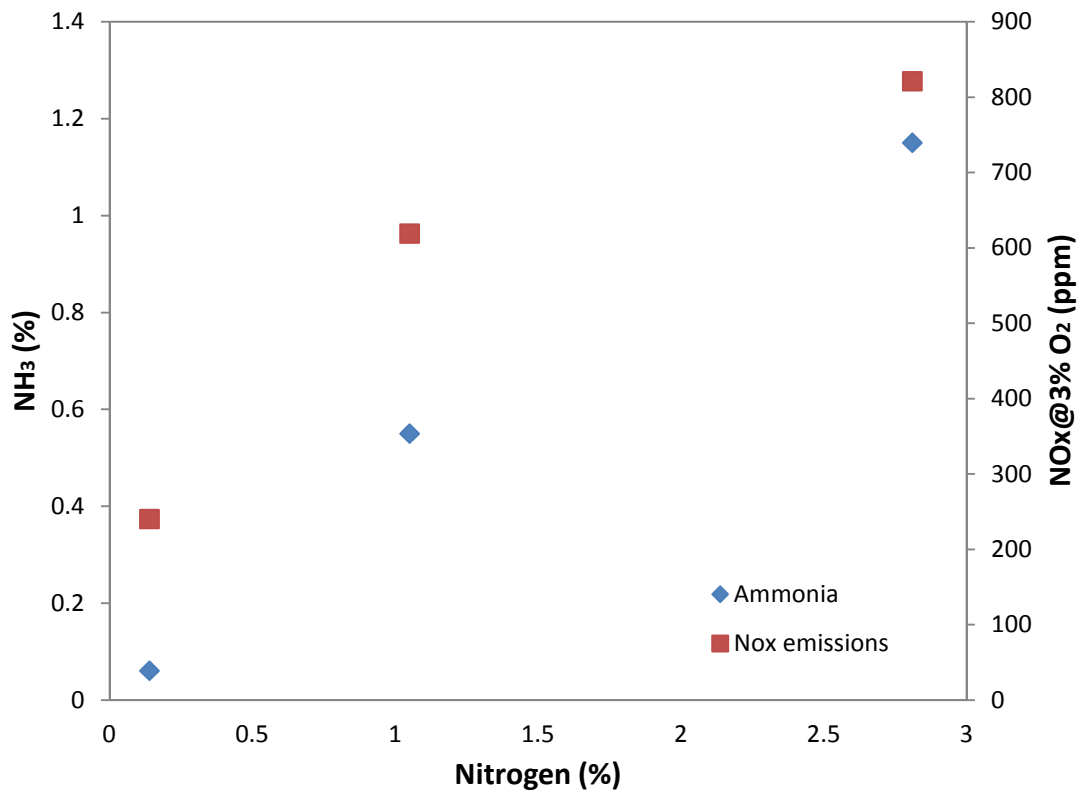


**Fig 4.11 - Relation of nitrogen content, ammonia, and NO<sub>x</sub> emissions for producer gas flow rate of 150 pph and equivalence ratio of 1.65**

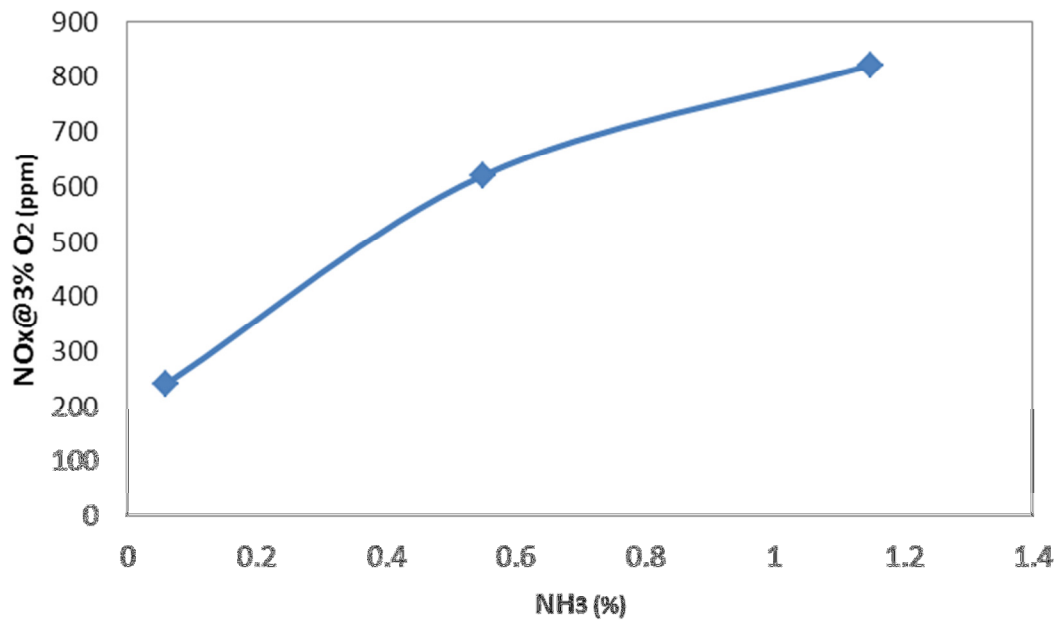


Fig 4.12 – NOx vs NH<sub>3</sub>

## CHAPTER 5: CONCLUSIONS AND RECOMMENDATIONS

### 5.1 Conclusions

Experiments were conducted on a pilot-scale biomass gasification and combustion system using different biomass feedstock. The feedstock vary mainly only in the nitrogen content, but ammonia concentrations in producer gas vary significantly, leading to vastly different NO<sub>x</sub> emission levels from the burner. It can be concluded that there is a direct relationship between the nitrogen content in biomass, ammonia in producer gas, and NO<sub>x</sub> emissions in the flue gas. It was found that fuel NO<sub>x</sub> accounts for a majority of the total NO<sub>x</sub> emissions when the biomass-derived producer gas is used. In the present setup, NO<sub>x</sub> emissions will reach a maximum level at lean conditions. At the same equivalence ratio, NO<sub>x</sub> emissions increase significantly as the heat rate increases due to the increase in the flame length and low residence time.

This study was able to establish the relationship between the nitrogen content in the biomass to the fuel NO<sub>x</sub> formation in the burner. The fuel NO<sub>x</sub> in this case seemed uninfluenced by the temperature (equivalence ratio) of the producer gas, mainly because of the characteristic of a diffusion flame. But its dependence on the heat rate was significant and is attributed to the ammonia content in the fuel. More ammonia in the fuel will enhance the effect of equivalence ratio on the NO<sub>x</sub> formation in the burner. Contrary to thermal NO<sub>x</sub>, the residence time seemed to be inversely proportional to the fuel NO<sub>x</sub> due to the presence of ammonia in the fuel.

## 5.2 Future recommendations

The overall objective of the project is to design a low NO<sub>x</sub> burner for fuels with nitrogen content. This would require a detailed understanding of the combustion and flame chemistry, especially for ammonia. Ammonia being the dominant nitrogen species in producer gas, the affinity of ammonia to various radicals under different conditions would give us a clear picture of NO<sub>x</sub> formation. Hence, a detailed chemical and computational analysis of non-premixed flames with a given producer gas composition would give us a better understanding of the flame and the NO<sub>x</sub> chemistry. These results could be compared to the experimental results to validate the computational model.

The ammonia capture using the IEA protocol is an effective way to ensure that all of the ammonia is accounted for. But this method is very time consuming. The setup of the impingers (a total of nine), followed by the collection and processing of the samples will amount to a minimum of 3-4 days. The use of a gas chromatography-mass spectrometer (GC-MS) or similar analytical instruments would have saved a lot of time, which could otherwise be used for extensive testing. The mass spectrometer was procured for this same reason, as it was known to have been successful in analyzing the producer gas composition for similar fluidized bed gasifiers. However, the present gasifier is a pressurized fluidized bed gasifier, which resulted in a large pressure drop when the producer gas entered the inlet capillary tube of the mass spectrometer, hence condensing water in some cases and clogging the capillaries with char coming at high pressures. In addition, the high moisture content and various contaminants also prohibited the

successful employment of GC-MS. If a convenient and accurate method for on-line ammonia measurement can be developed, more tests can be performed in a timely manner.

An experimental simulation of the gasifier setup, if replicated in a small scale with different ammonia seeding concentrations, would give options to explore more conditions to better understand the fuel NO<sub>x</sub> behavior. This will also reduce the development time for the low-NO<sub>x</sub> burner.

It would be advisable to run the producer gas in the burner with pure oxygen as the oxidizing agent, instead of air. This will eliminate nitrogen from atmospheric air, thus removing thermal NO<sub>x</sub> and focusing the study on fuel NO<sub>x</sub>, which is an essential part of this discussion. These results can then be compared to the air blown case, which will give a better understanding of the effects of different parameters on the fuel NO<sub>x</sub> formation. This will act as an important tool in the design of low NO<sub>x</sub> burner for fuels with nitrogen content.

## APPENDIX A1. ENGINEERING EQUATION SOLVER (EES) CODE

The following code is to calculate the flame temperature of the producer gas resulting from the gasification of yellow corn as the biomass feedstock. The EES code for the rest of the feedstocks are similar.

```
"
Tr = reactant temperature (K)
Tp = product temperature (K)
hr = reactant enthalpy (kJ/kmol)
hp = product enthalpy (kJ/kmol)
atom balances and first law of thermodynamics is used to find adiabatic flame temperature

mf_n2*N2+mf_co*CO+mf_h2*H2+mf_co2*CO2+mf_ch4+mf_c2h6*C2H6+mf_c2h4*C2H4+mf_c2h2*
C2H2+mf_c3h8*C3H8+mf_nh3*NH3+mf_h2o*H2O +
a(O2+3.76N2) --> d N2+b CO2+c H2O

"

"composition"
mf_n2 =39.02/100*1
mf_co =16.91/100*1
mf_h2 =11.33/100*1
mf_co2 =13.56/100*1
mf_ch4 =5.27/100*1
mf_c2h6 =0.26/100*1
mf_c2h4 =1.18/100*1
mf_c2h2 =0.07/100*1
mf_c3h8 =0.07/100*1
mf_nh3 =0.06/100*1
mf_h2o =09.97/100*1

"check sum"
sum_molef_check =
mf_n2+mf_co+mf_h2+mf_co2+mf_ch4+mf_c2h6+mf_c2h4+mf_c2h2+mf_c3h8+mf_nh3+mf_h2o

"atom balance"
d = a*3.76+mf_n2+mf_nh3/2
b = mf_co+mf_co2+mf_ch4+2*mf_c2h6+2*mf_c2h4+2*mf_c2h2+3*mf_c3h8
2*c = 2*mf_h2+ 4*mf_ch4+6*mf_c2h6+4*mf_c2h4+2*mf_c2h2+8*mf_c3h8+2*mf_h2o
a = b+c/2-mf_co/2-mf_co2-mf_h2o/2

"elemental composition for hpflame"
nC= b
nH = c
nO=2*b+c-2*a
nN=2*d-3.76*2*a
```

**"reactant properties"**

Tr = 298.15

a\_act = a

Pr = 1.013e5 [Pa]

**"reactant enthalpy"**

hrn2=ENTHALPY(N2,T=Tr)

hrco=ENTHALPY(CO,T=Tr)

hrh2 = ENTHALPY(H2,T=Tr)

hrco2=ENTHALPY(CO2,T=Tr)

hrch4=ENTHALPY(CH4,T=Tr)

hrc2h6=ENTHALPY(C2H6,T=Tr)

hrc2h4=ENTHALPY(C2H4,T=Tr)

hrc2h2=ENTHALPY(C2H2,T=Tr)

hrc3h8=ENTHALPY(C3H8,T=Tr)

hrnh3=ENTHALPY(AMMONIA,T=Tr,P=Pr)

hrh2o=ENTHALPY(H2O,T=Tr)

hro2=ENTHALPY(O2,T=Tr)

hrefco2=ENTHALPY(CO2,T=Tr)

hrefh2o=ENTHALPY(H2O,T=Tr)

hrefn2=ENTHALPY(N2,T=Tr)

**"product enthalpy"**

hpco2=ENTHALPY(CO2,T=Tp)

hph2o=ENTHALPY(H2O,T=Tp)

hpn2=ENTHALPY(N2,T=Tp)

**"net reactant enthalpy, used for LHV"**

h\_reac =

(mf\_n2+3.76\*a)\*hrn2+mf\_co\*hrco+mf\_h2\*hrh2+mf\_co2\*hrco2+mf\_ch4\*hrch4+mf\_c2h6\*hrc2h6+mf\_c2h4\*hrc2h4+mf\_c2h2\*hrc2h2+mf\_c3h8\*hrc3h8+mf\_nh3\*hrnh3+mf\_h2o\*hrh2o+a\*hro2

**"energy balance"**

h\_reac = d\*hpn2+b\*hpco2+c\*hph2o

LHV = h\_reac - (d\*hrefn2+b\*hrefco2+c\*hrefh2o)

## BIBLIOGRAPHY

- Agrawal, S.K.A.a.A.K., Experimental study of combustion of hydrogen-syngas/ methane fuel mixtures in a porous burner. *International Journal of Hydrogen Energy*, 2008. 33(4): p. 14407-1415.
- Babu, S. P., 2006. Workshop No. 1: Perspectives on biomass gasification. *IEA BioEnergy Agreement Task 33: Thermal Gasification of Biomass*, 1 - 46.
- Bergman, P. C. A., Paasen, S. V. B. V., Boerrigter, H., 2002. The novel 'OLGA' technology for complete tar removal from biomass producer gas. *Pyrolysis and Gasification of Biomass and Waste*, Strasbourg, France.
- Boocock., A.V.B.a.D.G.B., *Science in Thermal and Chemical Biomass conversion 1*: p. 235-267.
- Cassman, K. G., 2007. Food and fuel for all: realistic or foolish? *Biofuels, Bioproducts & Biorefining*, 1, 18-23.
- Chen, G., Andries, J., Spliethoff, H., Fang, M., Enden, P. J. V., 2007. Biomass gasification integrated with pyrolysis in a circulating fluidized bed. *Solar Energy* 76, 345-349.
- Chun-Zhu Li, L.L.T., Formation of NO<sub>x</sub> and SO<sub>x</sub> precursors during the pyrolysis of coal and biomass. Part 3. Further discussion on the formation of HCN and NH<sub>3</sub> during pyrolysis. *Fuel*, 2000. 79: p. 1899-1906.
- Darvell, L. I., 2006. Fundamentals and environmental aspects in the thermochemical conversion of biomass-PhD Thesis. School of Process, Environmental and Materials Engineering. University of Leeds.
- Faaij, A., 2006. Modern biomass conversion technologies. *Mitigation and adaptation strategies for global change*, 11, 343-375.
- Fu-Jun Tian, J.Y., Lachlan J. McKenzie, Jun-ichiro Hayashi, and Chun-Zhu Li, Conversion of Fuel-N into HCN and NH<sub>3</sub> During the Pyrolysis and Gasification in Steam: A Comparative Study of Coal and Biomass. *Energy Fuels*, 2007. 21(2): p. 517-521.
- Good, J., Ventress, L., Knoef, H., Zielke, U., Hansen, P. L., Kamp, W. V. D., Wild, P. d., Coda, B., Passen, S. V., Kiel, J., 2005. Sampling and analysis of tar particles in biomass producer gases - Technical Report, International Energy Agency, Paris, France.
- Glarborg, P., Jensen, A.D., Johnsson, J.E., 2003. Fuel nitrogen conversion in solid fuel fired systems. *Progress in Energy and Combustion Science*, 29, 89 - 113.
- P. Hasler, T.N., Gas cleaning for IC engine applications from fixed bed biomass gasification. *Biomass and Bioenergy*, 1999. 16: p. 385 - 395.
- Koger, S., Bockhorn, H., 2005. NO<sub>x</sub> formation from ammonia, hydrogen cyanide, pyrrole and caprolactam under incinerator conditions. *Proceedings of the Combustion Institute*, 30, 1201 - 1209.
- Jun Han, H.K., The reduction and control technology of tar during biomass gasification/pyrolysis: An overview. *Renewable and Sustainable Energy Reviews*, 2006. 12: p. 397-416.

- Kazuo Yamagishi, M.N., Terukazu Yoshie, Tsunenori Tokumoto, Yasuo Kakegawa, A study of NOx emission characteristics in two stage combustion.
- Krzysztof J. Ptasinski, Thermodynamic efficiency of biomass gasification and biofuels conversion. *Biofuels, Bioproducts and Bio-refining*, 2008. 2: p. 239-253.
- L. Athens & M. Claxton, R.T.W., Effect of fuel composition on emissions from ultra-low NOx burners. *American Flame Research Committee Fall International Symposium*, 1995.
- Leung, D.Y.C., Yin, X. L., Wu, C. Z., 2004. A review on the development and commercialization of biomass gasification technologies in China. *Renewable & sustainable energy reviews*, 8, 565-580.
- Li, C.-Z., Tan, L. L., 2000. Formation of NOx and SOx precursors during the pyrolysis of coal and biomass. Part 3. Further discussion on the formation of HCN and NH3 during pyrolysis. *Fuel*, 79, 1899-1906.
- Li, X. T., Grace, J. R., Lim, C. J., Watkinson, A. P., Chen, H. P., Kim, J. R., 2004. Biomass gasification in a circulating fluidized bed. *Biomass and Bioenergy*, 26, 171-193.
- Lv, P. M., Xiong, Z. H., Chang, J., Wu, C. Z., Chen, Y., Zhu, J. X., 2004. An experimental study on biomass air-steam gasification in a fluidized bed. *Bioresource technology*, 95, 95-101.
- Maniatis, K., 2001. Progress in Biomass Gasification: An Overview. *Progress in thermochemical biomass conversion*, 1, 1-31.
- McKendry, P., 2002. Energy production from biomass (part 1): overview of biomass. *Bioresource technology*, 83, 37-46.
- Nowacki, P., Coal Gasification Processes. *Energy Technology Review*; 70, 1981.
- Pershing DW, Wendt JOL. Pulverized coal combustion: the influence of flame temperature and coal composition on thermal and fuel NOx. *Proc Combust Inst* 1976; 16: 389–99
- Pinto, F., Andre, R. N., Gulyurtlu, I., 2009. Innovation on Biomass wastes utilization through gasification and co-gasification. Stage of deployment and needs for further R&D. *Biomass Gasification: Chemistry, processes and applications*. Nova Science Publishers, Inc, New York, pp. 7-69.
- Proll, T., Siefert, I. G., Friedl, A., Hofbauer, H., 2005. Removal of NH3 from biomass gasification producer gas by water condensing in an organic solvent scrubber. *Industrial & engineering chemistry research*, 44, 1576-1584.
- Ptasinski, K. J., Prins, M. J., Pierik, A., 2007. Exergetic evaluation of biomass gasification. *Energy*, 32, 568-574.
- Ragnar, W., Gasification of Biomass: comparison of fixed bed and fluidised bed gasifier. *Biomass and Bioenergy*, 2000. 18: p. 489-497.
- Reed, T. B., 2002. Encyclopedia of Biomass Thermal Conversion - The principles and technology of Pyrolysis, Gasification and Combustion. The Biomass Energy Foundation Press.

- Riquin Zhang, R.C.B., Andrew Suby, Keith Cummer. , Catalytic destruction of tar in biomass derived producer gas. *Energy Conversion and Management*, 2004. 45 (7-8): p. 995-1014.
- Sullivan, N., Jensen, A., Glarborg, P., Day, M.S., Grcar, J.F., Bell, J.B., Pope, C.J., Kee, R.J., 2002. Ammonia Conversion and NO<sub>x</sub> formation in Laminar co-flowing Nonpremixed Methane-Air Flames. The Combustion Institute, 285-298.
- Sung, C.-J.L., Chung. Fundamental Combustion Properties of H<sub>2</sub>/CO Mixtures: Ignition and Flame Propagation at Elevated Pressures. *Combustion Science and Technology*, 2008. 180(6): p. 1097-1116.
- Tian, F.-J., Yu, J., McKenzie, L. J., Hayashi, J.-i., Li, C.-Z., 2007. Conversion of Fuel-N into HCN and NH<sub>3</sub> During the Pyrolysis and Gasification in Steam: A Comparative Study of Coal and Biomass. *Energy Fuels*, 21, 517-521.
- Tijmensen, M. J. A., Faaij, A. P. C., Hamelinck, C. N., Hardeveld, M. R. M. V., 2002. Exploration of the possibilities for production of Fischer-Tropsch liquids and power via biomass gasification. *Biomass & Bioenergy*, 23, 129-152.
- Turns, S. R., 2000. An Introduction to Combustion : Concepts and Applications. McGraw Hill.
- Waibel, R. T., 1993. Ultra low NO<sub>x</sub> burners for industrial process heaters. Second International Conference on Combustion Technologies for a Clean Environment. John Zink, Lisbon, Portugal, pp. 1-15.
- Wang, L., Wellerb, C. L., Jonesb, D. D., Hanna, M. A., 2008. Contemporary issues in thermal gasification of biomass and its application to electricity and fuel production. *Biomass & bioenergy*, 32, 573-581.
- Wang, M.R.Y.a.T., Simulation of Producer Gas Fired Power Plants with Inlet Fog Cooling and Steam Injection. *J. Eng. Gas Turbines Power*, 2007. 129(3): p. 637 (11 pages)
- Q-Z Yu, C.B., G-X. Chen, K. Sjoström. , The fate of fuel-nitrogen during gasification of biomass in a pressurized fluidized bed gasifier. *Fuel* 2007. 86: p. 611-618.
- Zhang, R., Brown, R. C., Suby, A., Cummer, K., 2004. Catalytic destruction of tar in biomass derived producer gas. *Energy Conversion and Management*, 45 995-1014.